TECHNISCHE UNIVERSITÄT WIEN

VIENNA UNIVERSITY OF TECHNOLOGY

DIPLOMARBEIT

Ordered equilibrium structures of soft particles in layered systems

Ausgeführt am Institut für
Theoretische Physik
der Technischen Universität Wien
unter der Anleitung von
Ao. Univ. Prof. Dipl.-Ing. Dr. G. Kahl

durch
Mario Kahn
Nörenach 37, 9772 Dellach im Drautal

23. Mai 2008

Abstract

Inspired by various work about confined condensed matter systems we investigate ordered equilibrium structures formed by soft particles, interacting via Gauss potential, that are confined betweeen two parallel hard walls of variable distance. Using search strategies that are based on ideas of genetic algorithms, the energetically most favourable particle arrangements are identified. We obtain a detailed phase diagram of the system, that includes transition lines between the emerging structures and the number of layers that the system forms between the walls. Inspired by experiments, we put particular effort to gain a deeper insight into the phase transition mechanisms, i.e., the buckling and the prism phase transition. Furthermore, very large wall distances are considered, where the transition from the confined system to the bulk system is investigated.

Contents

1. Introduction

The search for ordered equilibrium structures in condensed matter physics is one of the most impressing stories in the history of science. Already *Johannes Kepler* has given an important contribution in this field of research in the year 1611. In the monograph, entitled "Strena, Seu de Nive Sexangula" (A New Year's Gift of Hexagonal Snow) he suggested a hexagonal symmetry of snowflakes, leading to the known *Kepler conjecture* statement for closest packing of hard spheres [1].

Almost two centuries later, based on the work of *Nicolas Steno* about crystal symmetries [2], *René Just Haüy* suggested for the first time that crystals are a regular three-dimensional array of particles with a repeating unit cell along three directions that are, in general, not perpendicular. In the nineteenth century further work about symmetries of crystal structures was done by *Auguste Bravais et al* [3]. Due to the discovery of x-rays, by *Conrad Röntgen* in 1895, the theoretical prediction then could be verified by means of *x-ray diffraction*, pioneered by the remarkable work of *Lawrence Bragg* and his father *Henry Bragg* [4, 5]. Shortly afterward *Erwin Schrödinger* and others formulated the non-relativistic quantum mechanics in 1926. Together with *Bloch's theorem*, that characterizes the wavefunctions of electrons in a periodic potential, the basis for a theoretical description and for the predictions of ordered structures in sold state physics was formed. For this reason its triumphal procession could not be impeded.

Over many decades, most of the progress in condensed matter physics was made in the field of atomic (hard) matter. Only recently, soft matter has emerged as a rapidly developing new field. The term "soft" stems from the fact that the rigidity of soft matter against mechanical deformations is by many orders of magnitude smaller than that of atomic systems. The systems that belong to soft matter are difficult to circumscribe; they cover a large range of mesoscopically sized particles ($\sim 1nm - 1\mu m$) such as dendrimers, polymeres, or microgels, but also vesicles or membranes. Examples of such materials include biological substances (proteins, viruses, DNA), as well as industrial matrials like mesoscopic polymer-chains.

Often the interaction potential between soft particle potentials diverge only weakly, at the origin, or sometimes remain finite at full overlap of the particles. For a general overview see [6, 7, 8]. Similar as hard matter systems, soft matter systems, also solidify and arrange in periodic structures. In this thesis I investigate this procedure for a paticular class of systems, which is confined in one direction, formed thereby layers. The model, that we consider is the *Gaussian Core Model* (GCM), which approximates the effective interaction [9] between the centers of mass of two polymer chains, known as the Flory-Krigbaum potential [10].

Although the thermodynamic properties of crystalline solids can be calculated within concepts of different levels of sophistication, such as simple lattice sums [11], cell models [12, 13, 14, 15] or density functional theory [16, 17, 18, 19, 20], an approach, to optimize the search for stable crystal structures, is still missing. Basicaly this search can be formulated as an optimization problem.
The problem of finding maxima and minima of functions with respect to their variables is certainly one of the most important questions in maths. In the 17^{th} century *Leibnitz* and *Newton* developed the integral and differential calculus which has brought along a breakthrough in this topic. For the very first time finding the (local) minima or maxima of a function could be realized in an analytic way by calculating the first derivative. One might say that then the scientific field of *optimization strategies* was born. Ever since increasingly powerful techniques have been developed to solve optimization problems. Depending on the conceptual approach most of the strategies can be classified as *deterministic*, *stochastic*, and *heuristic* applications. Each of these strategies has both advantages and disadvantages in different applications. Therefore the decision which method to choose depends essentially on the specific problem. For example, methods like *steepest descent* or *simplex methods* are doomed to fail for NP (non deterministic polynomial time)-complete optimization problems [21]. A famous representative of NP-complete problems is the *traveling salesman*[1]. In this thesis ordered equilibrium structures of soft particles are identified, a task which reduces to an *energy minimization* problem. To identify the energetically most favorable particles arrangements, search strategies which are based on ideas of *genetic algorithms* (GAs) will be applied. The work presented here dwells on the remarkable founding work of *Dieter Gottwald* [22, 23].

In recent years soft matter systems have been investigated in the bulk phase in exper-

[1]The general form of the traveling salesman problem has been first studied by mathematicians, during the 1930s in Vienna and at Harvard, notably by Karl Menger.

iment or in theory [24, 23, 25, 26, 27]. The situation gets more intricate when systems in confining geometries are considered. Due to the absence of periodic boundary conditions, in at least one direction, the identification of ordered equilibrium structures becomes possibly even more complex than in the bulk.
Remarkable experimental work on this topic was done by Pansu *et al.* [28] and *Bechinger et al* [29], who investigated sequences of structural transitions of hard spheres in a layered confined systems. This thesis is dedicated to follow the same line, with a theoretical approach, with the aim to help to unveil this exciting behavior in nature.

The thesis is organized in the following chapters:

- Chapter 2 presents the pair interaction potential of a system as well as the parameter of the system.
- Chapter 3 gives an overview over genetic algorithms, the basics of statistical mechanics, and lattice structures.
- Chapter 4 specifies how genetic algorithms can be applied to search for ordered equilibrium structures of minimal energy in condensed matter physics, whereby the implementation for a layered system will be described in detail.
- Results are presented in chapter 5; a detailed phase diagram of the system with the emerging structures will be provided. Furthermore, the three-dimensional bulk limit and the buckling mechanism will be discussed.

2. The Model

The system which I consider in this thesis are N soft particles in a volume V, which is confined by two parallel horizontal walls separated by a distance D; in this volume the particles arrange in n_l ordered layers. To describe the interaction between the particles the Gaussian core model (GCM) is used. Calculations are carried out for variable distance D and number-density $\rho = N/V$ at temperature $T = 0$. At zero temperature the free energy F reduces to the internal energy E which can be calculated via the lattice sum.

2.1. The Gaussian Core Model

The Gaussian core model (GCM) is a standard model system within the class of ultra-soft bounded potentials. Particular for *bounded* potentials is the fact, that they remain finite for the whole range of interaction distances. This holds even at zero separation, i.e., at full overlap between particles. In the context of atomic systems such potentials violate the Pauli principle, where full particle overlap is forbidden due to the repulsion between the electrons. Nevertheless the GCM has become a realistic model for a particular class of mesoscopic macro-molecules such as ploymer chains: For example, the effective interaction between two polymer chains can be approximated very well by the GCM, as has been confirmed in several studies, e.g. by *Krüger et al.* [30]. There, $\Phi_{\mathrm{GCM}}(r)$ represents a reliable form of the *effective interaction*, between the centers of mass of two such macromolecules.

The GCM was introduced originally by Frank H. Stillinger in 1976 [31]; its interaction potential is given by

$$\Phi_{\mathrm{GCM}}(r) = \epsilon e^{-(\frac{r}{\sigma})^2}. \tag{2.1}$$

The parameter ϵ defines the energy scale and σ defines the length scale. Furthermore, the system is characterized by a number density ρ. In general we use standard reduced units, i.e., $\rho^* = \rho\sigma^3$. Its potential $\Phi(r)$ is depicted in figure 2.1.

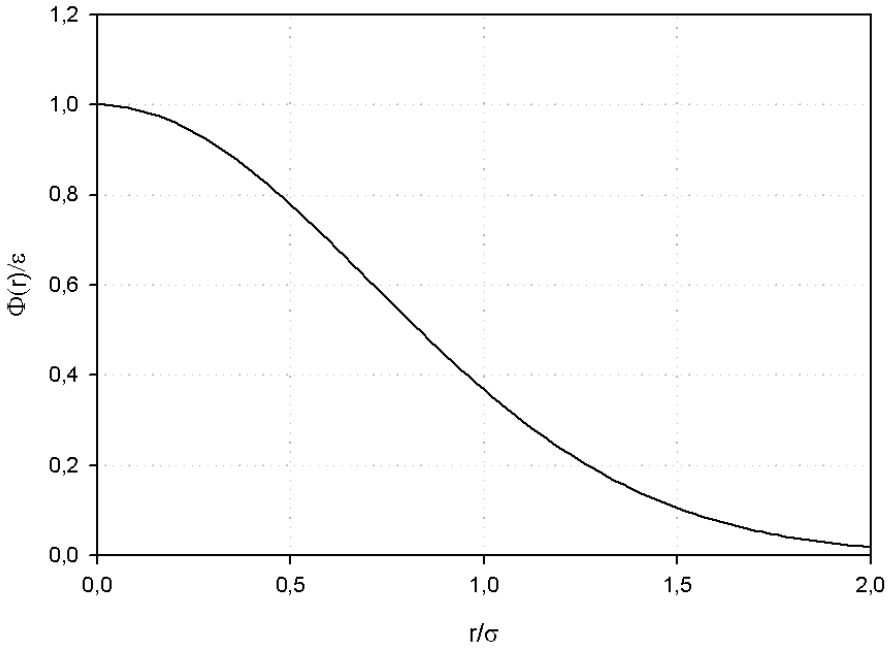

Figure 2.1.: The interaction potential $\Phi_{\mathrm{GCM}}(r/\sigma)$, of the Gaussian Core Model (GCM) as a function of r/σ.

Phase diagram Meanwhile, the phase diagram of the GCM bulk system is very well documented; its determination has been first carried out by Stillinger [31, 32, 33] and later in detail by A. Lang *et al* . [34]. It is depicted in figure 2.2.

Important for the present work is the isobar at $T = 0$. The detailed calculations of [34] reveal the following: At low temperatures the *fcc* structure is favoured, for $0.1794 \leq \rho^* \leq 0.1798$ an *fcc* and a *bcc* phase coexist, while for $\rho^* > 0.1798$ the GCM solidifies in a *bcc* structure.

2.2. The Layered System

2.2.1. The System

The system I investigate in this thesis are Gaussian particles immersed in a volume confined by two horizontal walls separated by a distance D. We consider ordered equilibrium structures of minimum energy. The system consists of n_l layers parallel

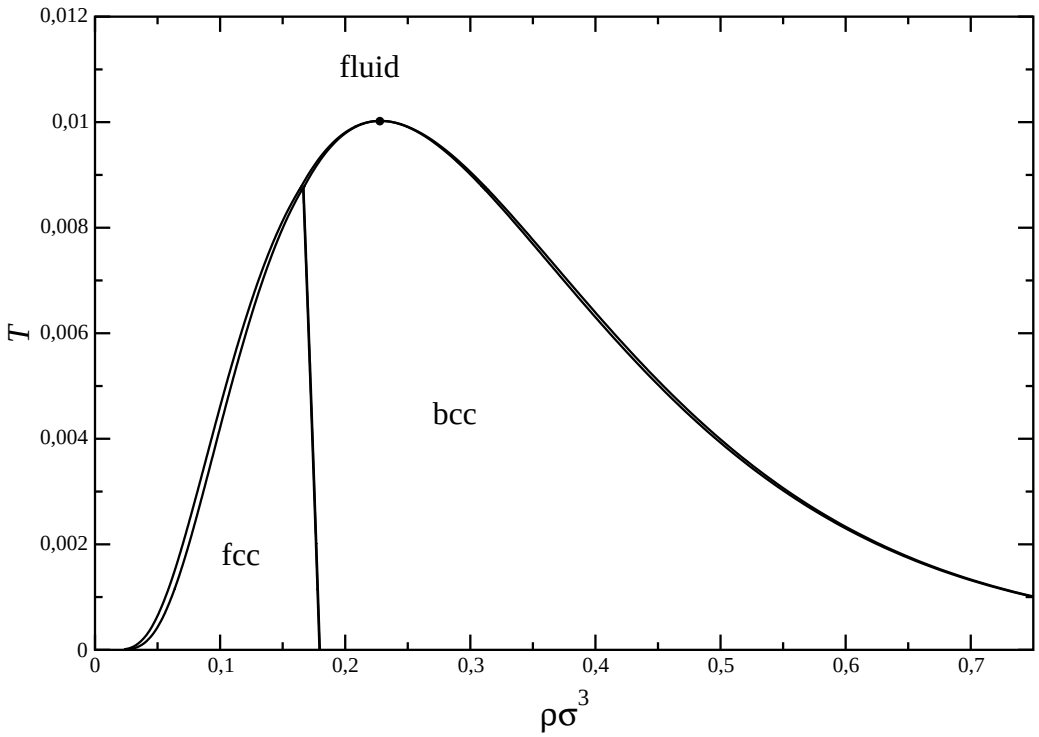

Figure 2.2.: The phase diagram of the GCM in the $T - \rho$ space, where T is in units of $k_B T$; taken from [34].

to the confining walls, which are assumed to lie in the (x, y)-plane and are thus perpendicular to the z axis. The layers are parallel to each other and all of them are assumed to have the same two-dimensional lattice structure. The parametrization of the ordered structures within the layers will be described in section 2.2.2. The origins of two neighbouring layers are connected via so called inter-layer vectors $\mathbf{c}_i$ with $i = 1, \ldots, n_l - 1$. Thus the inter-layer vector $\mathbf{c}_i$ connects the origins of the i-th layer to the one of the $(i + 1)$th layer, i.e., of two equivalent two-dimensional structures.
The z components of all inter-layer vectors sum up to the distance D.

Walls: To avoid misunderstandings concerning the walls, it is necessary to emphasise that in fact, we identify the first ($i = 1$) and the last layer ($i = n_l$) as the confining walls. For this reason no *wall-particle interactions* are considered in this thesis. Thus D denotes the distance between the first and the last layer.

Density: We distinguish between the bulk number density ρ and the area number density η. The relation between these two parameters is given via

$$\eta = \frac{\rho D}{n_l}. \tag{2.2}$$

2.2.2. Parametrization

Two-dimensional lattice: The two-dimensional lattice in each layer is described via two primitive vectors $\mathbf{a}$ and $\mathbf{b}$. They are parametrized via the ratio $x = |\mathbf{b}|/|\mathbf{a}|$ and the angle φ between them. $\mathbf{a}$ and $\mathbf{b}$ can therefore be expressed via:

$$\mathbf{a} = a \begin{pmatrix} 1 \\ 0 \end{pmatrix}, \quad \mathbf{b} = a \begin{pmatrix} x \cos\varphi \\ x \sin\varphi \end{pmatrix} \tag{2.3}$$

with the constraints

$$0 \leq x \leqslant 1, \quad 0 < \varphi \leqslant \pi/2. \tag{2.4}$$

I emphasize that the representation of the lattice via the vectors $\mathbf{a}$ and $\mathbf{b}$ is not unique. Above parametrization ensures that $\mathbf{a}$ is the largest vector. Its length, $a = |\mathbf{a}|$ is given via:

$$a = \left(\frac{n_b}{\eta x \sin\varphi} \right)^{1/2}, \tag{2.5}$$

where n_b is the number of basis particles in the unit cell. a is measured in units of σ.

Basis particles: Additional particles in the unit cell can be located at positions $\mathbf{B}_i$, with $i = 1, \ldots, n_b$. Without loss of generality the basis vector of the first particle is given as

$$\mathbf{B}_1 = \begin{pmatrix} 0 \\ 0 \end{pmatrix}.$$

For the other basis particle ($2 \leq i \leq n_b$) the representations of the $\mathbf{B}_i$ are given as linear combinations of the primitive vectors, i.e.,

$$\mathbf{B}_i = \alpha_i \mathbf{a} + \beta_i \mathbf{b} \qquad i = 2, \ldots, n_b,$$

with the constraints

$$0 \leqslant \alpha_i < 1, \quad 0 \leqslant \beta_i < 1. \tag{2.6}$$

This parametrization ensures that all particles lie within the primitive cell.

Inter-layer vector: As introduced above the displacement between two, neighbouring layers is characterized via the vectors $\mathbf{c}_i$, $i = 1, \ldots n_l - 1$. The setup is visualized in figure 2.3. The $\mathbf{c}_i$ are parametrized as follows:

$$\mathbf{c}_i = \alpha_i^c \mathbf{a} + \beta_i^c \mathbf{b} + h_i \begin{pmatrix} 0 \\ 0 \\ 1 \end{pmatrix} \qquad i = 1, \ldots, n_l - 1. \tag{2.7}$$

The vertical distance between two neighbouring layers is parametrized via the h_i, which have to fulfill the following constraints:

$$\begin{aligned} h_i &\geqslant 0 \qquad i = 1, \ldots, n_l - 1, \\ \sum_{i=1}^{n_l - 1} h_i &= D. \end{aligned} \tag{2.8}$$

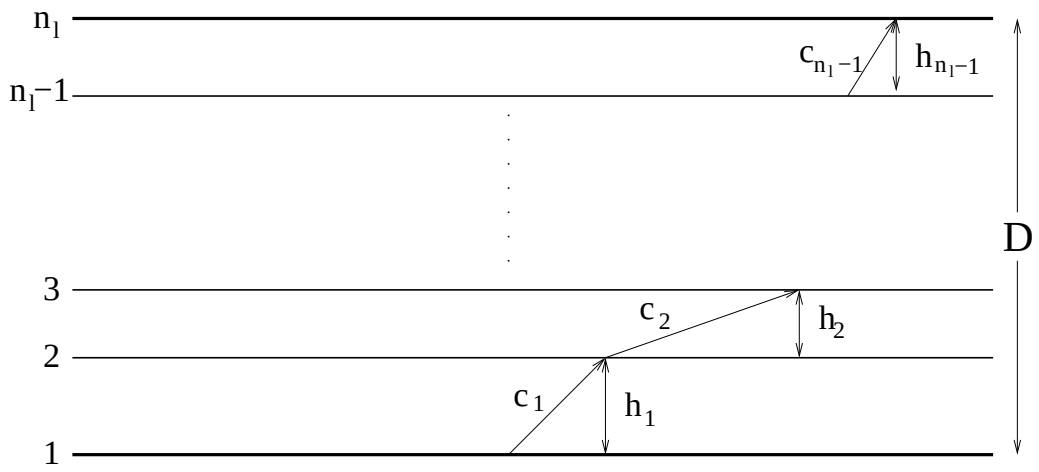

Figure 2.3.: *Sketch of a layered system.*

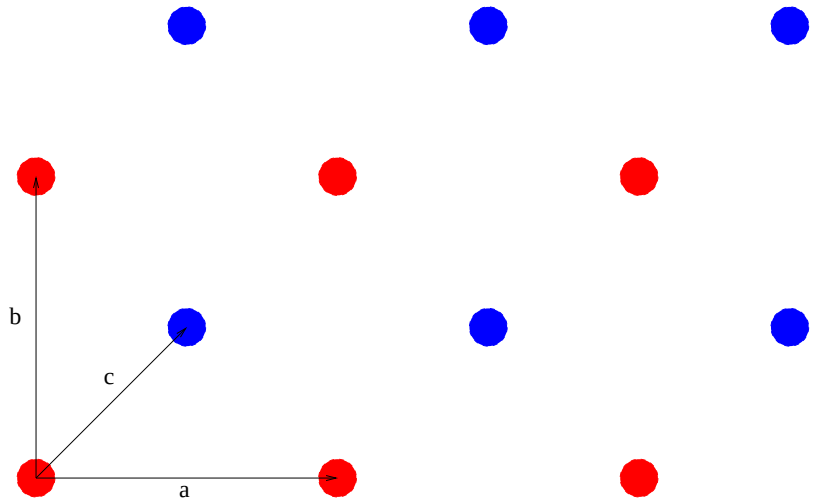

Figure 2.4.: Projection of a system with two layers onto the (x, y)-plane. **a** and **b** denote the primitve vectors, **c** is the interlayer-vector. Red particles belong to first and blue particle to the second layer.

3. Theory

3.1. Genetic Algorithms (GAs)

3.1.1. Introduction

Genetic algorithms: Genetic algorithms (GAs) are a subset of evolutionary algorithms. With respect to their search strategies, they belong to the stochastic search algorithms. GAs use features from natural evolutionary processes like survival of the fittest, reproduction and mutation, first described by Darwin [35]. The concept of GAs was introduced to engeneering problems by J.H. Holland in 1975 [36]. Further developments and improvements were carried out by Goldberg [37] and Michalewicz [38]. One benefit of genetic algorithms is that they search for globally optimized solutions. The danger to be trapped in locally optimal solutions is drastically reduced due to mechanisms, such as recombination and mutation. Another advantage of GAs is that they do not require derivatives of the function to be optimized. Therefore GAs are very effectiv in rough, complex search spaces. An interesting feature is the possibility to develop very fast and parallel implementations[1] of GAs [39, 40]. Nevertheless, GAs are not able to provide exact convergence to the optimal solution.

Though GAs were used successfully in various fields, such as for gene expression profiling analysis [39] or protein folding [41], they have not received due acknowledgement in physics for a long time. However, in recent years convincing evidence has been given that genetic algorithms are able to provide a powerful tool even in the field of condensed matter physics, i.e., laser pulse control [42] or cluster formation [43].

The genetic algorithm, that is used in this thesis, is fundamentally based on the work of D. Gottwald [22].

[1] The parallel feature is not implemented in this thesis

3.1.2. Basic Concepts

As in natural evolution, a *population* of individuals evolves in time, using principles such as inheritance, selection, recombination and mutation, towards better biological entities. Thus genetic algorithm use practically the same terminology as described as follows:

Data Representation

One of the main problems in implementation of evolutionary algorithms is the representation of the system variables, which shall be optimized during the GA. The different ways of encoding have been and still are widely discussed [44, 45]. In the following I will present the coding which is used in this thesis and I will describe furthermore some terms and definitions.

Gene: The most basic entity in GAs is the gene, its value is called *allele*. Allele can take the value of a certain alphabet $\mathcal{A} = \{a_1, \ldots, a_k\}$. In most cases the set of binary numbers is used as alphabet with $\mathcal{A}^{binary} = \{0, 1\}$. In this thesis we use the defintion where a single gene g_i takes the allele $[0, 1]$.
I have to mention that the definition of a gene in GAs is not unique, in some applications sequences of binary numbers are defined as genes.

Genetic divison: A genetic division[2] m_ξ is a series of genes g_i. In the section 4 I will identify a genetic division as the genetic encoding of one system parameter. $m_\xi \in [0, \ldots, 2^l - 1]$, with $\xi \in \{x, \varphi, \ldots\}$.

Genotype: The genotype is the encoded version of all parameters of a single candidate solution. Synonyms for the genotype are *chromosome* or *genome*.
Schematic representation of a genotype using the binary alphabet:

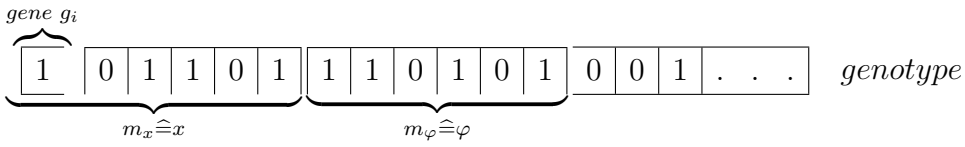

where x and φ are the system parameter of the two-dimensional layer (see section 2.2.2)

Phenotype or individual The phenotype stands for a candidate solution and represents therefore one point in search space. In this context a genotype is the

[2]The term "genetic division" is choosen by the author, there is no correspondent in the literature.

abstract representations of a phenotype. An interchangeably used synonym for phenotype is *individual*.

Population and generation: According to nature, we deal with sets of individuals, a so called population P. A population at a given time, or at its evolutional level, is called generation P_i, identified by the generation number i with $i = 0, \ldots, i_m$. The size of a population depends on the problem which is examined. Typically it contains several hundreds, sometimes thousands of individuals. The population size in each generation is constant.

Fitness: The fitness of an individual is a meassure for its quality. A higher fitness value indicates a better problem solution (see section 3.1.3).

3.1.3. Algorithm

As in the abiogenesis, the question of the origin of life, genetic algoritms start with a kind of primordial soup. The evolution starts from a population of randomly generated individuals, the generation with index $i = 0$. In each generation, the fitness of all individuals in the population is evaluated. Several individuals are statistically selected from the current population according to their fitness, forced to marry, to produce a new population. In each generation some individuals are "modified" by means of mutation. In the subsequent generations the newly created population forms the starting point of a new iteration, until a maximum number of generations has been produced or another termination condition is met.
In literature there exist many different, problem-depended, implementations of genetic algorithms but in their skeletal structure they ressemble each other. A *canonical* pseudo code for a genetic algorithm could read as:

begin
  i=0
  initialize($P(i)$)
  evaluate($P(i)$)
  while (**not** (termination-condition **or** imax)) **do**
    i=i+1
    fitness($P(i-1)$)
    $Q(i)$=*select*($P(i-1)$)
    $R(i)$=*recombine*($Q(i)$)
    $P(i)$=*mutate*($R(i)$)

evaluate$(P(i))$
done
end

The main parts of a genetic algorithms rest in the subroutines which are denoted in *italics*. The following section shall describe them in detail.

Initialization

Initially the individuals, i.e., solution candidates, of the first population are created randomly via stochastically distributed binary numbers. In general the random numbers are distributed *uniformly* in the entire search space but in some cases, it can be useful to "seed" the individuals in regions where optimal solutions are expected. In comparison to *Monte Carlo simulations* states could be weighted with $1/k_BT$.

Encoding

As a first step, the individual has to be encoded into its phenotype. This encoding procedure has to be *bijective* and therefore invertible.

Evaluation function

The evaluation function $g(\mathcal{I})$ assigns a number e_i to each individual $\mathcal{I}$. Therewith e_i is a measure for the qualitiy of $\mathcal{I}$. The evaluation number is problem dependent, see section 4.

Fitness function

The fitness, i.e., fitness for survival, of an individual is expressed via the so-called *fitness number* f. The fitness function $f(e_i)$ defines the probability that a single individual is chosen for reproduction. In general f is a function of $g(\mathcal{I})$. In many cases the distinction between the fitness and the evaluation is not made, therefore f becomes $f = e_i$. Although there are no special requirements on the fitness function it is commonly assumed that the fitness number is positive and that individuals with a higher fitness number have a higher probability to be selected for reproduction. Continuity or the strong causality to Rechenberg [45] is not *a priori* called for f.

The choice of the fitness function is problem-specific as well. Nevertheless there exist several "standard" functions, as listed below.

Linear fitness: The linear fitness function can be defined via $f_{\text{lin}} = 1/((\sum_{i=1}^{N} e_i) - e_i)$.

Proportional fitness: The most commonly used method is the proportional fitness function f_{prop} with $f_{\text{prop}} = e_i / \sum_{i=1}^{N_i} e_i$ where N_i is the number of individuals in the population. Thus individuals obtain a fitness proportional to their evaluation number e_i. (Compare the roulette wheel selection probability in the selection paragraph)

The fitness function, which is used in this thesis, will be introduced in section 4.

Constraints If the solutions have to fulfill a certain number of constraints it is advisable to consider them in the parametrization of the model or in the encoding transformation between genotype and phenotype. If this is not possible, individuals, that violate the constraints have to be suppressed in their propagation, by assigning a low fitness number (e.g. $f = 0$). That in turn leads to leads to convergence problems due to the fact that too many individuals have the same fitness number. To overcome this problem one can introduce a set of penalty functions $\psi_i(\mathcal{I})$ and associated weights r_i for each of the n constraints. The redefined fitness function f^* would then have the following form:

$$f^*(\mathcal{I}) = f(\mathcal{I}) - \sum_{i=1}^{n} r_i \psi_i(\mathcal{I}).$$

Selection

In the selection phase of the genetic algorithm the parents of subsequent populations will be chosen by a *selection method*. According to natural selection, individuals with higher fitness number, i.e., in this thesis individuals with higher e_i, will be preferred as parents. For the selection procedure exist different schemata have been proposed in the literature:

Linear Ranking Selection The selection probability of individuals does not depend on the fitness value itself. In fact it depends on the ranking of individuals according to their fitness. The ranking of an individual could be, e.g., the sort position according to their fitness. In the linear ranking method the number of offsprings, that the highest ranked individual is allowed to procreate, is

limited via a constant α_{max}. The number of offsprings for the subsequent individual, according to their quality, decreases linearly. This selection process prohibits that individuals with very high fitness number are chosen too often for reproduction.

Tournament Selection In this selection mode a few individuals contest in a "tournament": k individuals are selected at random from the population, the one with the highest fitness value wins the tournament and will be chosen for reproduction. With the value k the so called *selection pressure* can be adjusted. For smaller k values individuals with lower fitness have a higher probability to be selected for reproduction.

Roulette-Wheel Selection The roulette-wheel selection defines a selection probability proportional to the individuals fitness value. Thus individuals with a higher fitness value are preferred. The probability p_i that the i-th individual will be selected is given by

$$p_i = \frac{f(\mathcal{I}_i)}{\sum_{i=1}^{n} f(\mathcal{I}_j)}.$$

Similar as in the case of a roulette wheel each individual represents a slot on the wheel with a slot size appropriate to the selection probability. A pseudocode could read:

begin
  f=*fitness*$(P(i))$
  $\hat{f}$=*normalize*(f)
  $\bar{f}$=*accumulate*$(\hat{f})$
  i=1
  while (i **leq** N/2) **do**
    x=*random*(0,1)
    p1(i)=*find*(x,$\bar{f}$,$P(i)$)
    x=*random*(0,1)
    p2(i)=*find*(x,$\bar{f}$,$P(i)$)
  done
end

Here $\hat{f}$ is the probability density function and $\bar{f}$ the distribution function which are used to define the slot interval for each individual. The step *find* selects the first individual, for which $x \leq \bar{f}(\mathcal{I}_i)$ is valid, i.e. the first individual whose distribution function is greater than x.

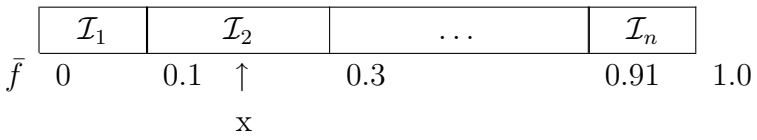

In literature the roulette-wheel selection is also known as *fitness proportional selection*.

For this thesis the roulette-wheel selection has been implemented and applied as the selection method.

Recombination

In this step the new population P_{i+1} is created through pairwise *crossover* of selected parents from the generation P_i. In each step two parents are combined to produce two new offspring. Thus a child solution typically shares many of the characteristic features of its parents.
Different recombination techniques are listed below and have been implemented:

- **One-point crossover**
  A single crossover point on both parent genotypes is determined at random. The genes at the left and at the right of that point are exchanged and recombined to form the childern; see figure 3.1.

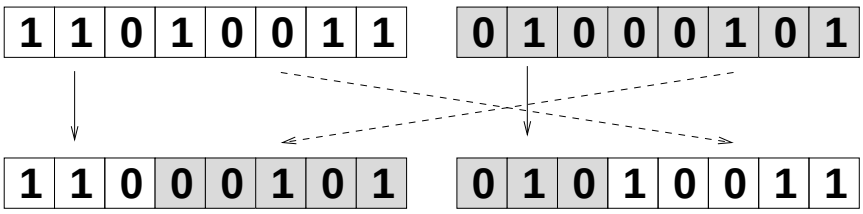

Figure 3.1.: Schematic representation of a one-point crossover process.

- **Two-point crossover**
  Two crossover points on both parent genotypes are determined at random. The genes located between these points are exchanged and recombined; see figure 3.2.

- **Random crossover**
  Several exchange points, represented via the exchange pattern X, on both parent genotypes are determined at random. Genes at positions with an according

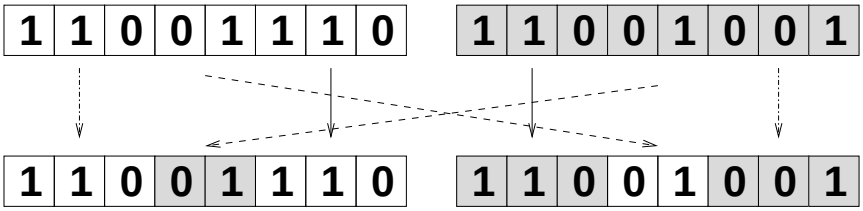

Figure 3.2.: Schematic representation of a two-point crossover process.

'0' in X remain unchanged and genes at positions with an according '1' in X are exchanged between the parents. In a technical notation the genes of the

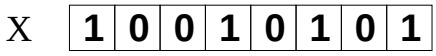

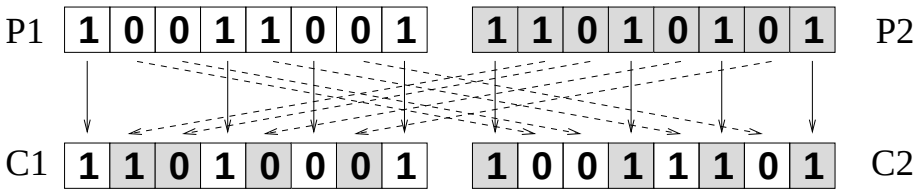

Figure 3.3.: Schematic representation of a random crossover process.

children are calculated via the following logical expressions:

$$C1 = (P1 \textbf{ AND } X) \textbf{ OR } (P2 \textbf{ AND } \textbf{ NOT } X)$$
$$C2 = (P2 \textbf{ AND } X) \textbf{ OR } (P1 \textbf{ AND } \textbf{ NOT } X)$$

For a schematic view see figure 3.3.

- **Random crossover with inversion**
  This method is similar to the random crossover, described above. However, there the second child is obtained from the first by exchanging '1's by '0' and vice versa. In a technical notation the genes of the two children are calculated via the following logical expression:

$$C1 = (P1 \textbf{ AND } X) \textbf{ OR } (P2 \textbf{ AND } \textbf{ NOT } X)$$
$$C2 = \textbf{ NOT } C1$$

  For a schematic view see figure 3.4.

In this thesis random crossover and random crossover with inversion have been applied.

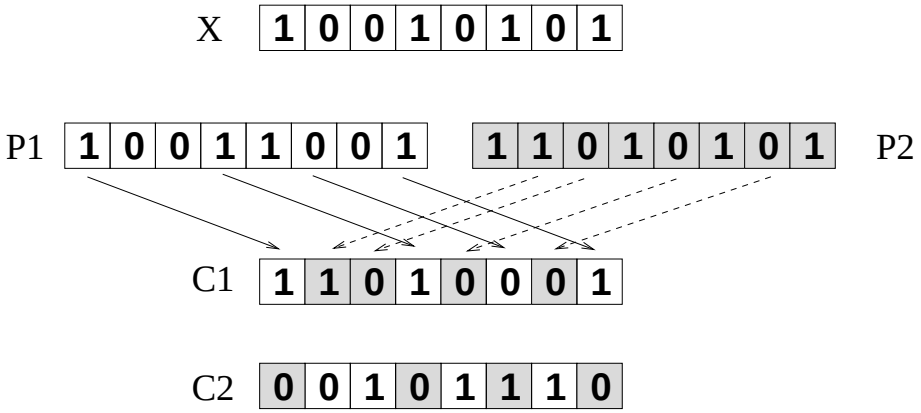

Figure 3.4.: Schematic representation of a random crossover procedure with inversion.

Mutation

In analogy to biology mutation, genetic algorithms use mutation to keep genetic diversity from one generation to the next and avoids inbreeding as well. Mutation should occur rather rarely, the probability p_{mutate} for a gene to mutate, is about 0.5%. Gene mutation cause a change of the allele to another value of the alphabet $\mathcal{A}$.

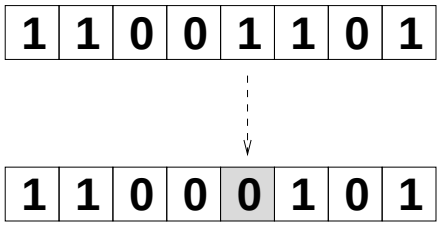

Figure 3.5.: Schematic represenation of a mutation of a gene.

Convergence

Genetic algorithms are not deterministic, since they use stochastic numbers to find the optimum solution. Thus genetic algorithm do not converge in the sense of:

$$||x_{k+1} - x^*|| \leqslant C||x_k - x^*||^p. \tag{3.1}$$

$||.||$ measures the distance, which is problem depended, between the exact problem solution x^* and the approximate solution x_i in the i-th iteration step, whereas $C > 0$ and $p > 0$.

3.2. Statistical Mechanics

In this chapter I shall give a brief introduction into the principles of statistical mechanics required for this thesis. The aim is to show how the free energy F, as all-dominant element in this thesis, can be derived from the microscopic particle behaviour. A comprehensive introduction to the subject can, for instance, be found in references [46, 47].

3.2.1. Basic Concepts

On a microscopic level, the state of a thermodynamic system consisting of N particles, is given via the particle positions $\mathbf{x} = \{x_1, \ldots, x_N\}$ and their momenta $\mathbf{p} = \{p_1, \ldots, p_N\}$. At a given time, these quantities are combined to $\mathbf{z}_t$ which represents one particle in the $6N$-dimensional phase space Π. Under the influence of *Newton's laws*, the particle positions and momenta evolve in time $\mathbf{z}_0 \rightarrow \mathbf{z}_t$, via the *Hamilton equations of motion*:

$$\frac{\mathrm{d}}{\mathrm{d}t}\begin{pmatrix}\mathbf{p}_t\\ \mathbf{x}_t\end{pmatrix} = \frac{\mathrm{d}}{\mathrm{d}t}\mathbf{z}_t = \sigma\frac{\partial H}{\partial \mathbf{z}}(\mathbf{z}_t) = \sigma\begin{pmatrix}\frac{\partial H(\mathbf{z}_t)}{\partial p}\\ \frac{\partial H(\mathbf{z}_t)}{\partial x}\end{pmatrix} \tag{3.2}$$

with

$$\sigma = \begin{pmatrix}0 & -1\\ 1 & 0\end{pmatrix} \tag{3.3}$$

and the *Hamiltion function* H for conservative systems:

$$H(\mathbf{z}_t) = \mathbf{p}^2/2m + V(\mathbf{x}); \tag{3.4}$$

$V(\mathbf{x})$ denotes the potential and $\mathbf{z}_0$ represents the particle's initial condition at $t = 0$

Ensemble

A statistical ensemble is resented by a large number of trajectories $\mathbf{z_t}$ in phase space. While each trajectory differs from each other, due to different initial conditions, they all refer to the same macroscopic, thermodynamic state of the system. Different macroscopic external constraints lead to different types of ensembles. For instance in the *microcanonical ensemble*, the system is characterized by fixed volume V, particle number N, and energy E.

In the *canonical ensemble* we consider systems of N particles confined in a volume V at constant temperature T. Therefore sometimes it is called the NVT-ensemble. To keep the system at constant temperature, it is considered to be in contact with a heat-bath with temperature T.

Partition functions

The partition function allows the calculation of thermodynamic properties out of the microscopic behaviour of the particles. Each statistical ensemble is characterized by its own partion function:

The microcanonical partition function Using the microcanonical *distribution function* f_E, that gives the probability for a given state $\mathbf{z}$ in phase space, the microcanonical partition function can be written as follows:

$$f_E(\mathbf{z}) = \delta(H[\mathbf{z}] - E) \tag{3.5}$$

with

$$Z(N, V, E) = \int_{\Pi} f_E(\mathbf{z}) \mathrm{d}z, \quad \Pi = \Pi(V, N) \tag{3.6}$$

The canonical partition function In the canonical ensemble, the partion function is given by

$$Z(N, V, T) = \int_{\Pi} f_T(\mathbf{z}) \mathrm{d}z \tag{3.7}$$

with the canonical distribution function

$$f_T(\mathbf{z}) = \exp\left\{-\frac{H(\mathbf{z})}{k_B T}\right\}. \tag{3.8}$$

where k_B is the *Boltzmann's constant* and the entropy $S = k_B \Phi^{(3)}$. The link between the microcanonical and the canonical ensemble is given via:

$$Z(N, V, T) = \int_{-\infty}^{+\infty} Z(N, V, N) \exp\left\{-\frac{E}{k_B T}\right\} \mathrm{d}E \tag{3.9}$$

$$= \int_{\Pi(V,N)} f_T(\mathbf{z}) \mathrm{d}z \tag{3.10}$$

In this thesis, we have used the canonical ensemble.

For the sake of completness, in literature the partition function appears very often with another prefactor, namely $\hbar^{-3N}/N!$, where $\hbar = h/2\pi$ is the *Plank constant* and $N!$ accounts for the in-distinguishability of the particles. Because prefactors only are relevant for the evaluation of distribution functions, they have no relevance for ensemble averages.

Observable

The connection between the microscopic description within statistical mechanics and the macroscopic physical properties, is realized via averages over *observables*. With the time evolution of $\mathbf{z}_t$ the observable $A(\mathbf{z}_t)$ changes along the trajectory. To obtain a macroscopic quantity for A one has to calculate the *time average* $\langle A \rangle_t$ along the time evolution of $\mathbf{z}_t$. Under the assumption of *ergodicity*, the trajectory passes each point in phase space; with this hypothesis (which actually connot be proven) the average is identical to the so called *ensemble average*:

$$\langle A \rangle_E = \frac{1}{Z} \int_\Pi A(z) f(\mathbf{z}) d\mathbf{z}. \tag{3.11}$$

Thermodynamic potentials

All thermodynamic properties of the system are completely determined by the thermodynamic potentials. They can be calculated via suitable partial derviatives from the according potentials with respect to their natural variables. Each ensemble type has its according thermodynamic potentials Φ. Analogous, to the situation, in changing from one partion function to another, thermodynamic potentials can be transformed mutually via the so called *Legendre transformation*.

For historical reasons, thermodynamic potentials are not represented via their Φ^i, for instance $\Phi^{(1)}$, the potential of the canonical ensemble, is represented via the *internal energy* E, with the transformation:

$$k_B \ln Z(N,V,E) = k_B \Phi^1(N,V,E) = S(N,V,E) \tag{3.12}$$

$$\Rightarrow E = E(S,V,N) \tag{3.13}$$

3.2.2. Free Energy

For the canonical ensemble the appropriate thermodynamic potential is the *Helmholz free energy*. It contains the total information about the thermodynamic properties of the system in the canonical ensemble and is given as a function of its natural variables N,V, and T via

$$F(N,V,T) = -k_B T \ln Z(N,V,T). \tag{3.14}$$

All other thermodynamic properties can be calculated via suitable derivative of F with respect to its variables. Between T and the internal energy E, the following relationship is given:

$$E = F - TS. \tag{3.15}$$

In this thesis I consider only systems at zero temperature, thus $F = E$. For an ordered system the latter is given by the lattice sum.

3.2.3. Lattice Sum

The *lattice sum* is the sum over all interactions between the particles arranged in an ordered lattice. Thus the internal energy E for a simple lattice, i.e., a lattice with just one basis particle, is given by

$$E = \frac{1}{2} {\sum_{\{\mathbf{R}_i\}}}' \Phi(R_i) \tag{3.16}$$

where $\{\mathbf{R}_i\}$ is the set of all lattice positions and $\Phi(r)$ is the pair potential between the particles; the prime indicates that the term $\mathbf{R} = (0,0,0)$ is omitted. For a three-dimensional lattice with the primitive vectors $\mathbf{a}$, $\mathbf{b}$ and $\mathbf{c}$ the lattice sum can be written as

$$E = \frac{1}{2} {\sum_{ijk}}' \Phi(|i\mathbf{a} + j\mathbf{b} + k\mathbf{c}|) = \frac{1}{2} {\sum_{ijk}}' \Phi(|\mathbf{v}_{ijk}|). \tag{3.17}$$

where the $\mathbf{v}_{ijk}$ denote the lattice vectors.

Lattices with basis particles require an additional term in the lattice sum, i.e.,

$$E = \frac{1}{2} {\sum_{ijk}}' \Phi(|\mathbf{v}_{ijk}|) + \frac{1}{n_b} \sum_{ijk} \sum_{l>m}^{n_b} \Phi(|\mathbf{v}_{ijk} + \mathbf{B}_m - \mathbf{B}_l|). \tag{3.18}$$

where $\mathbf{B}_l$ and $\mathbf{B}_m$ represent the basis particle positions within the primitve cell.

The lattice vectors $\mathbf{v}_{ijk}$, considered in this thesis are given by:

$$\mathbf{v}_{ijk} = i\mathbf{a} + j\mathbf{b} + \sum_{g=1}^{k-1} \mathbf{c}_g \tag{3.19}$$

where k is the number of the layer with index k and where $\mathbf{c}_g$ is the inter-layer vector as given in equation (2.7).

Furthermore, the free energy per particle at zero temperature of the considered system, is given by

$$\frac{F}{N} = \frac{E}{N} \tag{3.20}$$

Thus the search problem in this thesis is to find appropriate values for the basis vectors $\mathbf{a}$, $\mathbf{b}$ and $\mathbf{c}_g$ such that the lattice sum has the lowest free energy.

As the system is built up via two-dimensional layers, a brief introduction into the expected two-dimensional *Bravais lattices* is given in the following.

3.3. Two-dimensional Bravais Lattices

This section gives an overview about the five existing two-dimensional Bravais lattices. The parametrization is the one introduced in section 2.2.2; it is, of course, not unique.

The following two-dimensional bravais lattices are represented via the vectors $\mathbf{a}$, $\mathbf{b}$ and the angle *phi* between them.

3.3.1. Square lattice

Primitive vectors:

$$\mathbf{a} = \begin{pmatrix} a \\ 0 \end{pmatrix} \quad \mathbf{b} = \begin{pmatrix} 0 \\ a \end{pmatrix}$$

$|\mathbf{a}| = |\mathbf{b}|$ and $\varphi = \pi/2$.

Area of the unit cell:

$$A_c = a^2$$

The symmetry operation of the square lattice is a four-fold rotation axis.

3.3.2. Hexagonal lattice

Primitive vectors:

$$\mathbf{a} = \begin{pmatrix} a \\ 0 \end{pmatrix} \quad \mathbf{b} = \begin{pmatrix} a/2 \\ \sqrt{3}a/2 \end{pmatrix}$$

$|\mathbf{a}| = |\mathbf{b}|$ and $\varphi = \pi/4$

Area of the unit cell:

$$A_c = \frac{\sqrt{3}a^2}{2}.$$

The symmetry operation of the square lattice is a six-fold rotation axis.

3.3.3. Rectangular lattice

Primitive vectors:

$$\mathbf{a} = \begin{pmatrix} a \\ 0 \end{pmatrix} \quad \mathbf{b} = \begin{pmatrix} 0 \\ b \end{pmatrix}$$

$|\mathbf{a}| \neq |\mathbf{b}|$ and $\varphi = \pi/2$.

Area of the unit cell:

$$A_c = ab$$

The symmetry operations of the square lattice are two perpendicular mirror axes.

3.3.4. Centered Rectangular lattice

Primitive vectors:

$$\mathbf{a} = \begin{pmatrix} a \\ 0 \end{pmatrix} \quad \mathbf{b} = \begin{pmatrix} a/2 \\ b/2 \end{pmatrix}$$

$|\mathbf{a}| \neq |\mathbf{b}|$ and $\varphi = \pi/2$.

Area of the unit cell:

$$A_c = \frac{ab}{2}$$

The symmetry operations of the square lattice are two perpendicular mirror axes.

3.3.5. Oblique lattice

Primitive vectors:

$$\mathbf{a} = \begin{pmatrix} a \\ 0 \end{pmatrix} \quad \mathbf{b} = \begin{pmatrix} b\cos\varphi \\ b\sin\varphi \end{pmatrix}$$

$|\mathbf{a}| \neq |\mathbf{b}|$ and $\varphi \neq \pi/2$.

Area of the unit cell:

$$A_c = ab\sin\varphi$$

The oblique lattice has no symmetry elements.

As we can see, the rectangular and the centered rectangular lattices posses the same symmetry elements and refer therefore to the same symmetry group. The table 3.1 gives an overview over all of the two dimensional Bravais lattices.

Square	Hexagonal
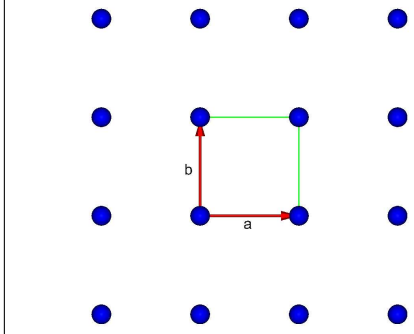	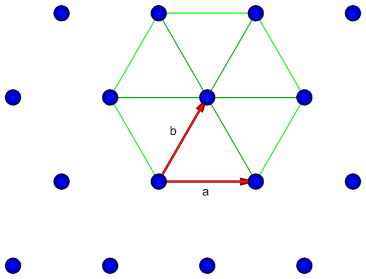
Rectangular	Centered Rectangular
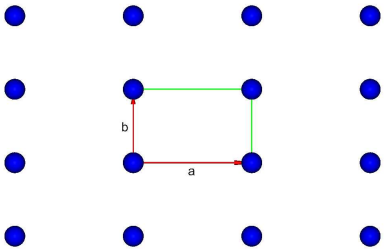	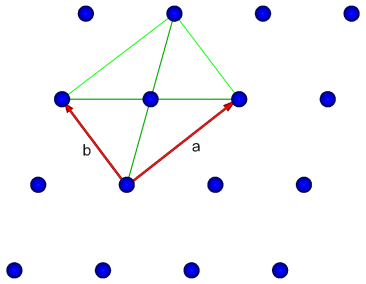
Oblique	
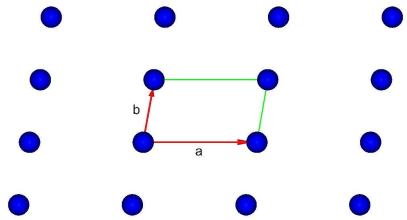	

Table 3.1.: Bravais lattices in two dimensions.

4. Implementation of the GA

This section contains details how the genetic algorithm is implemented for the problem of a layered system. Part of the implementation was already done by Dieter Gottwald [22].

4.1. GA in layered systems

The genetic algorithm, that is implemented in this thesis, encodes the system parameters, as described in section 2.2.2, in the individuals. The ensemble dependent fitness function is designed in such a way that individuals evolve to solutions with lower energies. At the end the final result is improved via a steepest descent algorithm.

It has to be mentioned, that strictly speaking, the implemented algorithm is a modified version of real genetic algorithms. The best solution is the best solution in the last generation. In our algorithm, generally this is not the case. Instead, we retain the best solution during all generation steps and take it as the final result.

4.1.1. Data representation

The system parameter $\{x, \varphi, \alpha_2, \dots\}$ are encoded in a genetic division, represented as an integer number with length l_a and l_n which denote the parameter length for numbers and angles. Thus, the accuracy of the representation of each parameter can be varied via these two quantities. The maximum length of a genetic division is delimited by 32, i.e., the length of an integer variable in the memory. The parameter range of m_φ lies between $[0, \dots, 2^{l_a} - 1]$, all other parameter lie between $[0, \dots, 2^{l_n} - 1]$. It has to be pointed out, that this data representation leads to a discrete search space with its advantages and disadvantages.

Decoding and Encoding

The decoding and encoding method defines the mapping between system parameter in real space and their corresponding binary representation m_ξ. This mapping can be realized in different ways, e.g., one can do a non-uniform mapping, in a way that regions, where solution of system parameter are expected, are convered with higher density. This refers directly to the convergence behaviour of the genetic algorithm. For *hard spheres* and a *square shoulder* systems progressive work is currently done by *Gernot Pauschenwein* [48]. Nevertheless, the encoding in this thesis has to fullfill the constraints given in equations (2.4) and (2.6).

The decoding function is the inverse of the encoding function.

4.1.2. Lattice Unification

The representation of a given lattice via primitive vectors is not unique. This leads to infinitely many different but equivalent sets of primitive vectors that describe exactly the same lattice. The same ambiguity problem is encountered in the choice of basis vectors for $n_b > 1$. The following strategies, developed by Dieter Gottwald shall help to solve this problem partly.

Primitive Vectors

To avoid ambiguities we chose primitive vectors with respect to a minimal circumference of the primitive cell, spanned by the two vectors $\mathbf{a}$ and $\mathbf{b}$. The following iterative algorithm is applied:

1. Start with the two primitive vectors $\mathbf{a}^*, \mathbf{b}^*$.
2. Calculate Σ^*, which prepresents the circumference of the primitve cell, spanned by $\mathbf{a}^*, \mathbf{b}^*$.
3. Assemble the following four sets of the primitive vectors:

$$\begin{array}{cc} (\mathbf{a}^* + \mathbf{b}^*, \mathbf{b}^*) & (\mathbf{a}^*, \mathbf{b}^* + \mathbf{a}^*) \\ (\mathbf{a}^* - \mathbf{b}^*, \mathbf{b}^*) & (\mathbf{a}^*, \mathbf{b}^* - \mathbf{a}^*). \end{array}$$

4. Calculate, for each of the above sets $\tilde{\Sigma}$, i.e. the circumference of the corresponding unit cell.

5. If for one of the four sets $\tilde{\Sigma}$ is smaller than Σ^* the corresponding sets represents the new set of primitive vectors, the algorithm is terminated.

6. Start again with step 1 while $\tilde{\Sigma}$ of one of the four sets is smaller than Σ^*.

Basis Vectors

For the case that there are more than one basis particles we also have to deal with a further ambiguity: The indices of the basis vectors $\mathbf{B}_i$ can be permuted without changing the lattice. To overcome these ambiguities certain constraints on the basis vectors have to be imposed. In this work the following strategy was applied:

1. Create the sets
$$\{\tilde{\mathbf{B}}_i^{(j)}\} = \{\mathbf{B}_i - \mathbf{B}_j\}, \qquad j = 1, \ldots, n_b$$
with
$$\begin{aligned} \tilde{\alpha}_i^{(j)}\mathbf{a}^* + \tilde{\beta}_i^{(j)}\mathbf{b}^* &= \tilde{\mathbf{B}}_i^{(j)} \\ \tilde{\alpha}_i^{(j)} &= \bar{\alpha}_i - \bar{\alpha}_j \\ \tilde{\beta}_i^{(j)} &= \bar{\beta}_i - \bar{\beta}_j. \end{aligned}$$

2. Calculate
$$\begin{aligned} \alpha_i^{(j)} &= \tilde{\alpha}_i^{(j)} - [\tilde{\alpha}_i^{(j)}] \\ \beta_i^{(j)} &= \tilde{\beta}_i^{(j)} - [\tilde{\beta}_i^{(j)}] \end{aligned}$$
where $[x]$ denotes the largest integer smaller or equal x. Thus the resulting values of $\alpha_i^{(j)}$ and $\beta_i^{(j)}$ lie in the interval $[0, 1)$.

3. Calculate $\Upsilon^{(j)}$ via
$$\Upsilon^{(j)} = \sum_{i=1}^{n_b} (\alpha_i^{(j)} + \beta_i^{(j)})$$
and find $\Upsilon^{(j^*)} = \min\{\Upsilon^{(j)}\}$.

4. Sort B_i^* first in ascending order by $\alpha_i^{(j^*)}$, then in ascending order by $\beta_i^{(j^*)}$. This ensures that the vector basis vector $B_1^* = (0, 0)$ will always be first.

5. Calculate the new basis particle coordinates $\mathbf{B}_i^*$ with the new uniquely defined set of basis vectors via

$$\mathbf{B}_i^* = \alpha_i^{(j^*)}\mathbf{a}^* + \beta_i^{(j^*)}\mathbf{b}^*, \qquad i = 1, \ldots, n_b.$$

Vector orientation

In general the set of primitive vectors $\mathbf{a}$ and $\mathbf{b}$, that emerge from lattice unification algorithm, do not match with the parametrization presented in section 2.2.2. Therefore, if necessary, the orientation of the vectors has to be modified with the following algorithm.

1. Order vectors via their magnitude so that $|\mathbf{a}| \geq |\mathbf{b}|$.
2. Rotate vectors that $\mathbf{a}$ is parallel to the x-axis and $\mathbf{b}$ lies in the x-y-plane.
3. Inversion of the vectors if necessary

The vector orientation necessitate the solution of equation

$$\bar{\alpha}_i\mathbf{a}^* + \bar{\beta}_i\mathbf{b}^* = \mathbf{B}_i$$

to obtain valid basis particle parameters $\bar{\alpha}_i$ and $\bar{\beta}_i$. Additionally, the same operation has to be performed for the interlayer-vectors $\mathbf{c}_i$, i.e., for the α_i^c and β_i^c.

The steps during the vector orientation are depicted in figure 4.1.

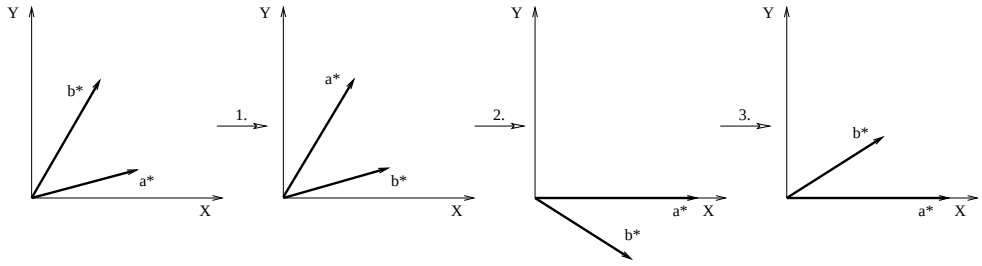

Figure 4.1.: *Steps of a new vector orientation*

Backward Projection into the Search Space

The primitive vectors $\mathbf{a}^*$, $\mathbf{b}^*$ and the basis vectors $\{\mathbf{B}^*\}$ are in general not any longer elements of the discrete search space due to modifications during the lattice

unification operation. Therefore it is necessary to project them onto the closest element of the finite binary representation, which can be performed as follows:

1. Calculate the system parameters x and y from of the primitive vectors $\mathbf{a}^*$, $\mathbf{b}^*$ via

$$x = \frac{|\mathbf{b}^*|}{|\mathbf{a}^*|}$$
$$\varphi = \arctan \frac{b_y^*}{b_x^*}.$$

   where b_x^* and b_y^* denote the x- and y-components of the primitive vector $\mathbf{b}^*$.

2. Encode parameter $\xi \in \{x, \varphi, \alpha_2, \dots\}$ in the corresponding genetic division m_ξ (see section 4.2.1).

3. Decode m_ξ again and calculate the corresponding primitive vectors $\mathbf{a}'$ and $\mathbf{b}'$.

4. The basis particle parameters α_i' and β_i' have to be adjusted, so that the binary values represent the closest real values of the parameters, as well. Therefore calculate new basis particle coordinates with equation:

$$\alpha_i'\mathbf{a}' + \beta_i'\mathbf{a}' = \mathbf{B}_\mathbf{i}^* \quad i = 2, \dots, n_b$$

   and do steps 2 and 3 for α_i' and β_i'.

5. Repeat the described procedure to project the parameters of the inter-layer vector c_i' onto the closest element of the finite binary representation.

4.1.3. Lattice Sum

Cutoff Radius For the cutoff radius r_{cut} we take the distance, beyond which the contribution to the lattice sum becomes smaller than some given ι and is defined via

$$F = \int_{r_{\text{cut}}}^{\infty} \Phi(r)\mathrm{d}r - \delta \int_0^{\infty} \Phi(r)\mathrm{d}r < \iota$$

A typical value for ι is 10^{-8} which leads to a typical cutoff-radius of approximately 4.3σ.

The lattice sum, presented in equations (3.18) and (3.19), is calculated via the following steps:

1. Set the *cutoff radius*. This is done only once.

2. Calculate the real space z-coordinates for each layer via the inter-layer vectors.
3. Going through all of the n_l layers, consider for the current layer those layers that are within the cutoff radius.
4. Calculate the value for the pair potential considering all distances between pairs of particles within the cutoff radius and sum them up.
5. To obtain the final free energy, divide the sum by n_l.

4.1.4. Steepest Descent

Since, the search space in genetic algorithms is discrete, due to the finite binary representation of the parameters, the accuracy of the resolution is limited. Thus the solution $\mathcal{I}^*$ proposed by the genetic algorithm lies, in general, close, but not exactly at the "true" solution. To account for this a multi-dimensional steepest descent hill climbing method has been applied [49].
We proceed as follows:

1. Decode the individual $\mathcal{I}^*$ to obtain the system parameters

$$\mathbf{q} = (x, \varphi, \alpha_2, \dots) \tag{4.1}$$

   where $\mathbf{q}$ identifies a complete parameter set and represents therefore an n_p-dimensional vector.

2. Set initial step size δ to

$$\delta = \left(\frac{1}{2}\right)^{\min\{l_n, l_a\}}. \tag{4.2}$$

3. For each system parameter ξ, with unit vector e_ξ, a small deviation $\mathbf{q}_\xi$ with stepsize δ, from the starting point $\mathbf{q}_\xi$ is calculated as follows:

$$\mathbf{q}_\xi \in \{\mathbf{q} \pm \delta \mathbf{e}_\xi\} \tag{4.3}$$

4. Calculate $F(\mathbf{q})$ and $F(\mathbf{q}^*) = \min\{F(\mathbf{q}_\xi)\}$.
5. If $F(\mathbf{q})$ is lower than $F(\mathbf{q}^*)$ then $\mathbf{q}$ is set to $\mathbf{q}^*$, otherwise δ will be decreased by a factor of 3.
6. Repeat with step 3., while $\delta > \delta_{\text{thresh}}$; here δ_{thresh} is a typical threshold of 10^{-10}. Otherwise the algorithm terminates.

The final crystal structure is then given by the last value of $\mathbf{q}^*$ with $F(\mathbf{q}^*)$ as the lowest free energy.

4.2. NVT Ensemble

In the NVT-ensemble for each run the wall distance D, the number of layers n_l and number the density ρ are fixed. As we consider ordered equilibrium structures, the parametrization in section 2.2.2 leads to following parameters in the NVT-ensemble.

4.2.1. Implementation of System Parameter

The parameters ξ that describe the NVT-ensemble are

$$\{x, \varphi, \alpha_2, \beta_2, \ldots, \alpha_{n_b}, \beta_{n_b}, \alpha_2^{\mathrm{c}}, \beta_2^{\mathrm{c}}, \ldots, \alpha_{n_l}^{\mathrm{c}}, \beta_{n_l}^{\mathrm{c}}, z_1, \ldots, z_{n_l-2}\}$$

where z_i (described below) is introduced for the simple reason of an easier implementation of the h_i with respect to the constraint given in equation (2.8). The relation between the h_i and tze z_i is then given by

$$\begin{aligned}
h_1 &= z_1 D \\
h_2 &= z_2 (D - h_1) \\
&\vdots \\
h_i &= z_i \left(D - \sum_{j=1}^{i-1} h_j \right) \\
&\vdots \\
h_{n_l} &= D - \sum_{j=1}^{n_l-1} h_j .
\end{aligned}$$

Since $z_i \in [0, 1), i = 1, \ldots, n_l - 2$, they can be encoded directly in the individual, without external constraints.

The total number of parameters n_p that are used to describe the crystal lattice is given by

$$\begin{aligned}
n_p &= 2 + 2(n_b - 1) + 2(n_l - 1) + n_l - 2 \\
&= 2n_b + 3n_l - 4.
\end{aligned}$$

Two parameters are used for x and φ, $2(n_b - 1)$ parameters to describe the basis particles without $\mathbf{B_0}$, $2(n_l - 1)$ parameter which denote the displacement in the (x, y)-direction, and $n_l - 2$ parameters which describe the displacement in the z direction.

Decoding and Encoding in the NVT-ensemble

The decoding method performes the transformation between the real space system parameter and the binary representation of the parameters in the NVT-ensemble. The decoding functions that fullfill the constraints of equations (2.4) and (2.6), can be written as

$$\begin{aligned} x &= \frac{m_x + 1}{2^{l_\mathrm{n}}} \\ \varphi &= \frac{\pi}{2}\frac{m_\varphi + 1}{2^{l_\mathrm{a}}} \\ \alpha_i &= \frac{m_{\alpha_i}}{2^{l_\mathrm{n}}} \\ \beta_i &= \frac{m_{\beta_i}}{2^{l_\mathrm{n}}} \\ \alpha_i^\mathrm{c} &= \frac{m_{\alpha_i^\mathrm{c}}}{2^{l_\mathrm{n}}} \\ \beta_i^\mathrm{c} &= \frac{m_{\beta_i^\mathrm{c}}}{2^{l_\mathrm{n}}}. \end{aligned}$$

The parameters l_a denote the length of the genetic division for angles and l_n for numbers.

An encoding function is the inverse of decoding function with an additional rounding of the m_ξ to the next integer

$$\begin{aligned} m_x &= round\left[x * 2^{l_\mathrm{n}} - 1\right] \\ m_\varphi &= round\left[\varphi * \frac{2}{\pi} 2^{l_\mathrm{a}} - 1\right] \\ m_{\alpha_i} &= round\left[\alpha_i 2^{l_n}\right] \\ m_{\beta_i} &= round\left[\beta_i 2^{l_n}\right]. \qquad (4.4) \\ m_{\alpha_i^\mathrm{c}} &= round\left[\alpha_i^\mathrm{c} 2^{l_n}\right] \\ m_{\beta_i^\mathrm{c}} &= round\left[\beta_i^\mathrm{c} 2^{l_n}\right]. \qquad (4.5) \end{aligned}$$

4.2.2. Evaluation Function

The evaluation function, in the NVT-ensemble, is given via the free energy per particle $F = E(x, \varphi, \alpha_2, \beta_2, \ldots, \alpha_{n_b}, \beta_{n_b}, \alpha_2^{\mathrm{c}}, \beta_2^{\mathrm{c}}, \ldots, \alpha_{n_l}, \beta_{n_l}, z_1, \ldots, z_{n_l-2})$ at temperature $T = 0$ as discussed above.

4.2.3. Fitness Function

As we search for crystal structures with the lowest free energy, lattices with lower energy are preferred. For this reason the fitness function increases with decreasing free energy. Our choice for the fitness function in the NVT-ensemble reads as

$$f(\mathcal{I}) = \exp\left(1 - \frac{F(\mathcal{I})}{F_{\mathrm{cubic}}}\right) \tag{4.6}$$

where $F(\mathcal{I})$ is the free energy per particle for the crystal structure represented by the individual $\mathcal{I}$, F_{cubic} is the free energy per particle of a cubic crystal structure.

5. Results

The aim of the investigations in this thesis is to study the ordered particle arrangements between two and three dimensional crystal structures. The volume is infinitely extended in the (x, y)-direction and confined in z direction by two horizontal walls. The first and last layers are located directly in the walls (for details see section 2.2.2). Since $T = 0$, the free energy reduces to the lattice sum. We assume, that the lattices in all layers are identic. All calculations where performed under the assumption, that the lattice in each layer is a simple lattice, i.e. $n_b = 1$. This assumption is based on detailed calculations that give evidence, that non simple lattices can be created via two or more layers of zero seperation (coinciding layers see section (5.2.1)).
This section is organized as follows:

- First, we will introduce the phase diagram of system as the main result in this thesis. This is done in an effort to provide a first overview over the results for the reader.
- Next, we present curves for the free energies as a function of D and ρ, on which the phase diagram is based.
- Then, the emerging structures, that appear in the phase diagram will be studied in detail and the transition from the confined volume into the bulk phase will be discussed. At last, we investigate and visualize the buckling transition mechanism for a transition where an arrangement of three layers becomes energetically more favourable than a two layer system.

5.1. Phase diagram

To identify the energetically most favorable particles arrangements we perform independent runs for each fixed layer number n_l and distance D, varying ρ^*. For a given density and distance, the system with the lowest free energy is considered to be the

stable structure. The calculations were performed on a grid with $\Delta\rho = 0.25\sigma$ and $\Delta D = 0.25$ varied from $D = \sigma$ to $D = 10\sigma$ and $\rho^* = 0.05$ to $\rho^* = 0.65$. The number of layers ranges from two to nine.

The phase diagram allows the location of the transition lines between the emerging structures and the number of layers that the system forms. The phase diagram in its simplest version, i.e., without identifying the emerging structure is depicted in figure 5.1, the phase diagram that allows to identify the emerging structure is depicted in figure 5.2.

5.1.1. Layer transition

At low distances $D \lesssim 3.5\sigma$ and for all densities, the system is characterized by two layers. Of course the area density increases at fixed n_l with increasing D due to the relation $\eta = \rho D/n_l$. Only if η becomes too high, the formation of a new layer can lower the energy and we observe a transition from an n_l to an $(n_l + 1)$-layer system.

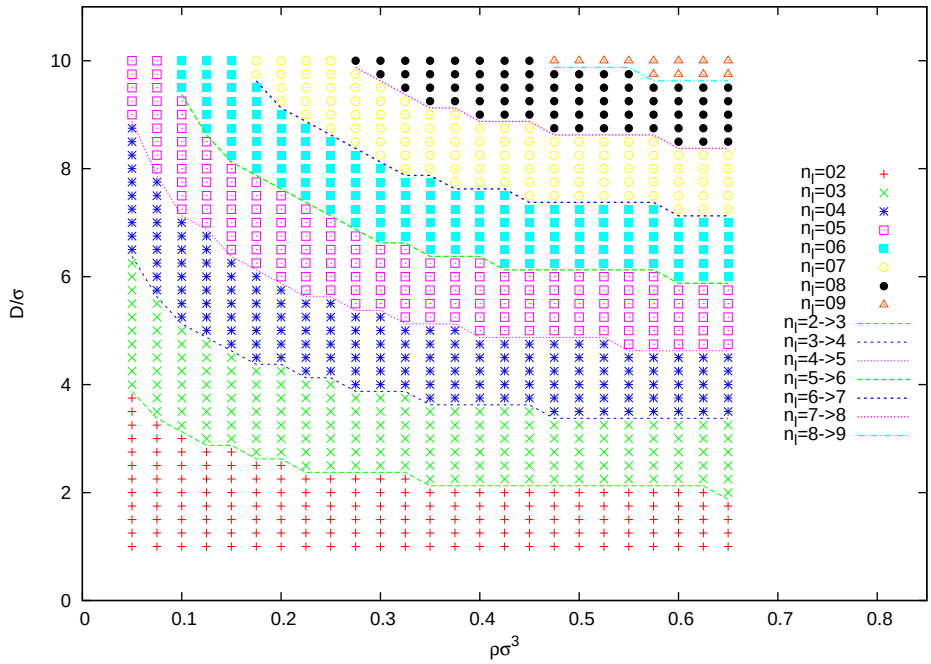

Figure 5.1.: Phase diagram of a system in (D, ρ^*)-space. Regions where the system forms n_l layers are identified. The lines are added as a guide to the eye.

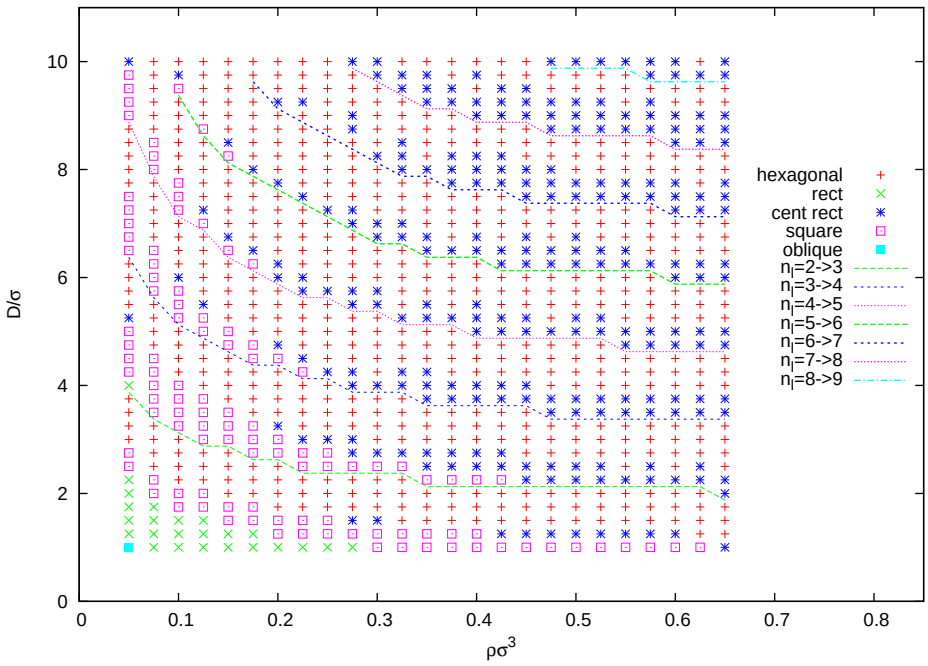

Figure 5.2.: Phase diagram of our system in $(D, \rho^*$-space. Regions where the system forms n_l layers are identified; lines are added as a guide to the eye. In addition, for each state point the corresponding stable structure is characterized by a symbol (see inset).

5.1.2. Structure transition

Structure transition for $\rho^* \sim 0.05$

Considering the system at a very low density $\rho^* = 0.05$ and at wall distance $D = \sigma$ all particles are separated by distances longer than the cutoff-radius $r_c \sim 4.3\sigma$. Thus the free energy of this configuration is lower than the numerical accuracy (10^{-8}) and is therefore considered to be zero.

With increasing D, a wide region is found, where a rectangular structure is stable, which then transforms to a square lattice at $\rho^* \sim 0.05$ and $D \sim 2.5\sigma$. At this densities we observe at fixed layer number n_l a sequence of square lattices, followed by an hexagonal lattice; sometimes an intermediate rectangular structure is observed.

The transition to a system with $(n_l + 1)$ layers is accompanied by the morphological transition which follows the well known transition relation [50]:

$$n_l\Delta \longrightarrow (n_l + 1)\square \longrightarrow (n_l + 1)\triangle \tag{5.1}$$

where n_l is the the number of layers, $\square$ and $\triangle$ correspond to layers of quadratic and hexagonal symmetry.

Considering the bullk system, that solidifies at this density into an *fcc* crystal, the sequence can be understood, via a closest packing scenario, considering the different ways to build up an *fcc* crystal via a stacking of layers. The height of an *fcc* stack with square (100) layers is smaller than that of the corresponding hexagonal (111) stack. Thus, with increasing cell height, the (100) stacked fcc structure fits first between the walls and is later replaced by the corresponding (111) phase in order to optimize the packing density.

Structure transition for $0.05 < \rho^* \leq 0.1$

Starting again at very small wall separation $D \sim \sigma$ and low volume-number densities $\rho^* \sim 0.075$, one can observe, with increasing D, the following sequence of two-dimensional Bravais lattices: First the lattice is rectangular, being followed by a square lattice via a continuous transformation, as has been confirmed via further calculations. For wall distances $D \gtrsim 2\sigma$ the particles arrange in a hexagonal lattice up to the layer transition line $2n_l \longrightarrow 3n_l$, at which a layer transition and a structural transition emerge simultaneously. Then, with further increasing D we observe a

sequence of two-dimensional Bravais lattices which starts from a square, followed by a hexagonal lattice; again, via a layering transition it becomes square. The situation is basically described via the following relation:

$$2\square \longrightarrow 2\square \longrightarrow 2\triangle \longrightarrow 3\square \longrightarrow 3r \longrightarrow 3\triangle \longrightarrow 4r \longrightarrow 4\triangle \ldots \tag{5.2}$$

where $\square$, $\square$, r and $\triangle$ correspond to layers of rectangular, quadratic, centered rectangular and hexagonal symmetry.

The sequence of appearing structures at $\rho^* = 0.1$ is similar to the situation at $\rho^* = 0.075$ where the structural behaviour is similar to the one, described above, with the exceptions of an intervening centered rectangular lattices at wall distances 6σ and 9.75σ.

Structure transition for $\rho^* \sim 0.2$

The phase region $0.2 \leq \rho^* \leq 0.3$ is similar to the situation with $\rho^* = 0.1$. First, for $n_l = 2$ and $D = \sigma$, the structure is rectangular which transform continuously to a square lattice. As the wall distance increases, the lattice structure becomes hexagonal until an additional layer is formed. Then the layers are built up by a square lattice structure again, followed by a centered rectangular lattice and a hexagonal layer. For $n_l > 3$ the square structure vanishes. This morphological transitions can be identified again as the transition relation, given in equation 5.2.

Structure transition for $0.3 \leq \rho^* \leq 0.4$

This region is similar to the region at $\rho \sim 0.2$ with the exception, that at small D-values the rectangular phase does not appear, but the system forms rather a square lattice.

Structure transition for $\rho^* > 0.5$

At such densities the bulk system solidifies in a *bcc* lattice. For $n_l > 2$ the square structure does not emerge any longer; we can identify a distinct transition from a square to a rectangular structure at $n_l = 2$. The sequence of transitions looks as follows:

$$2\square \longrightarrow 2r \longrightarrow 2\triangle \longrightarrow 3r \longrightarrow 3\triangle \longrightarrow 4r \longrightarrow 4\triangle \ldots \tag{5.3}$$

where $\square$, r and $\triangle$ correspond to layers of quadratic, centered rectangular and hexagonal symmetry.

Although the stacking of the appearing layers with their according structures do not correspond exactly to their respective bulk phase, the arrangement of the particles in the layers is strongly influenced by the stable bulk crystal structure but not completely dominated by it. For instance the centered rectangular Bravais structure, that hints to a *bcc* bulk phase, does in fact appear rather frequently at regions where the stable bulk phase solidifies in *bcc*.

The following two sections, where we consider in detail the energy curves and the structures, shall give a deeper insight into the results that were discussed above.

5.2. Free energies

In the following we present the reduced free energy per particle, $F/(N\epsilon)$, of a layered systems as a function of wall distance D and ρ. Each of the following figures, 5.3, 5.4, 5.5, 5.6, correspond to a diffent bulk density ρ^*. In each of these figures, the different curves correspond to a different number of layers n_l. These figures provide an insight, how the layer formation mechanism works. As the wall distance D increases, more particles have to arrange in each layer. However, a higher area densites causes an increase of the free energy per particle which can only be lowered by the insertion of a new layer. Therefore more and more layers appear in system as D increases.

5.2.1. Coinciding layers

The approach presented in section 2.2.2 allows to treat particular systems with different but equivalent parametrization. For instance, a system at a given state point that is composed by two layers, can equally well be parametrized, for instance, by four layers, where two pairs of layers have the same z-coordinate. This fact offers a good possibility to check the internal consistency of the approach, since both parametrizations should lead to the same energy.

In addition, the fact that our application allows coinciding layers offers the approach to study another intresting phenomena. Let us focus in figure 5.4 at the region $D \sim 3\sigma$. Here the curves for two and three layer arrangements are intersected by a curve of six layer arrangements that have a lower free energy. This gives evidence

for an additional phase, known in literature as buckling or prism phase, as suggested by Pansu *et al.* [28] and Bechinger *et al.* [29]. With respect to that result the phase diagram presented in figure 5.2 has to be modified. A more detailed discussion of this phenomena will be given in section 5.4.2.

5.2.2. Non monotonicity in the energy

For particular configurations [e.g. $\rho^* = 0.05, n_l = 3, D = 5.25\sigma$; $\rho^* = 0.05, n_l = 4, D = 7.5\sigma$ or $\rho = 0.10, n_l = 4, D = 6\sigma$], as depicted in figures 5.3 and 5.4, the energy shows as a function D a non monotonistic behaviour. These humps result obviously from a structural transition; a more detailed investigation shows that with increasing D the lattice structure is first centered rectangular, then hexagonal and then again centered rectangular. However, since the energy curves are expected to be concave, this might be a hint for a hidden structure, with even higher complexity at these state points. Additional calculations or another parametrization are necessary to verify this.

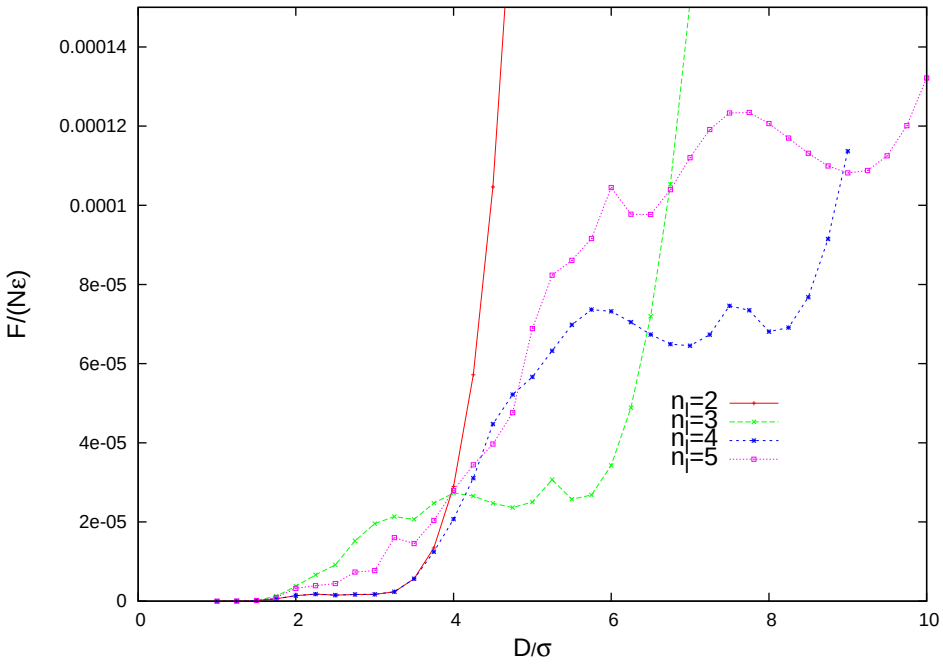

Figure 5.3.: $F/(N\epsilon)$ of a layered system at bulk density $\rho^* = 0.05$ vs. D/σ. Different curves correspond to different number of layers n_l (see inset).

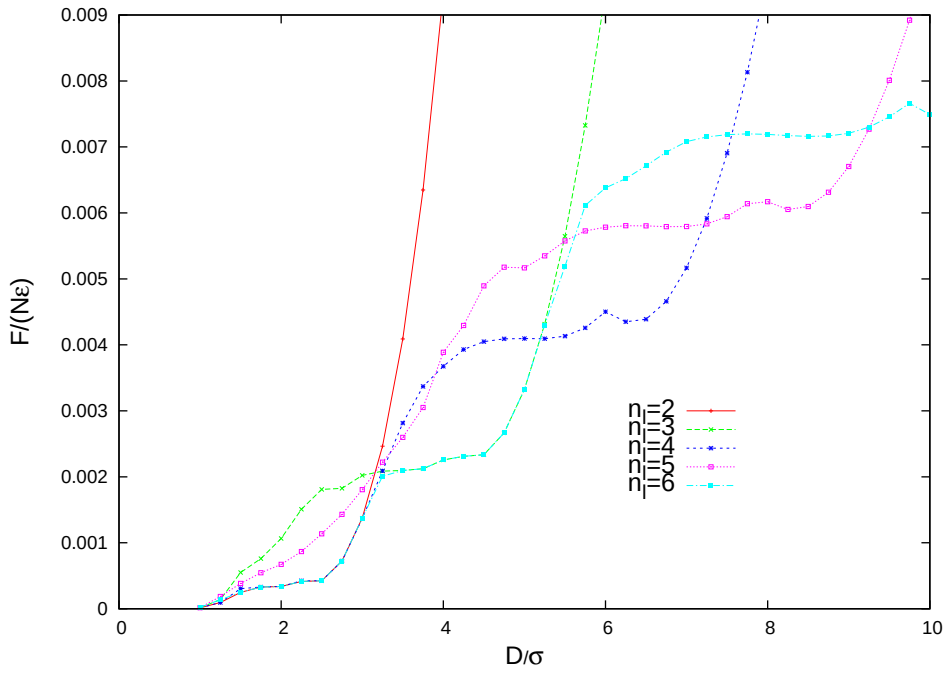

Figure 5.4.: $F/(N\epsilon)$ of a layered system at bulk density $\rho^* = 0.1$ vs. D/σ. Different curves correspond to different number of layers n_l (see inset).

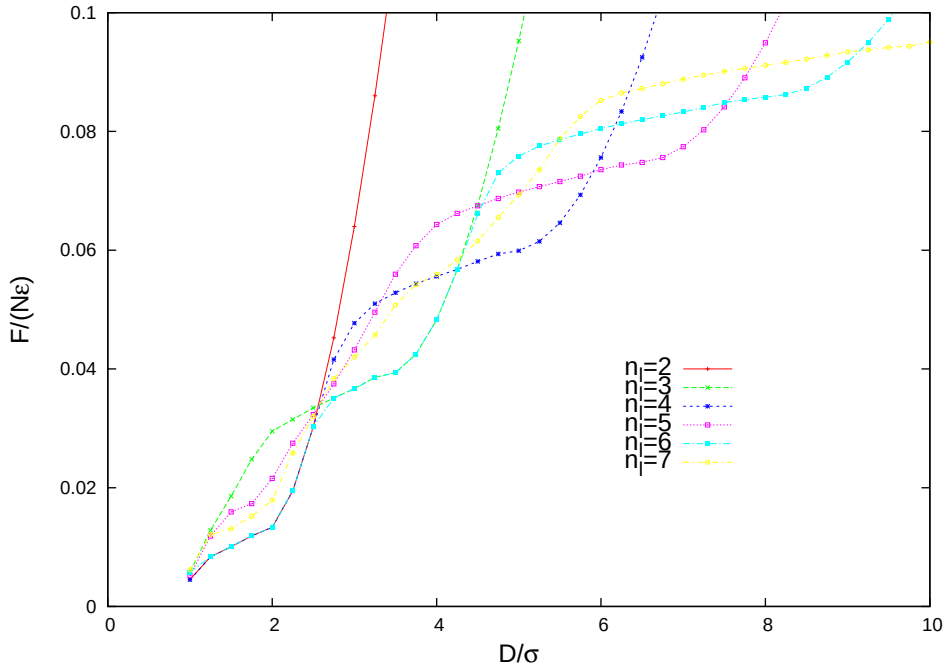

Figure 5.5.: $F/(N\epsilon)$ of a layered system at bulk density $\rho^* = 0.2$ vs. D/σ. Different curves correspond to different number of layers n_l(see inset).

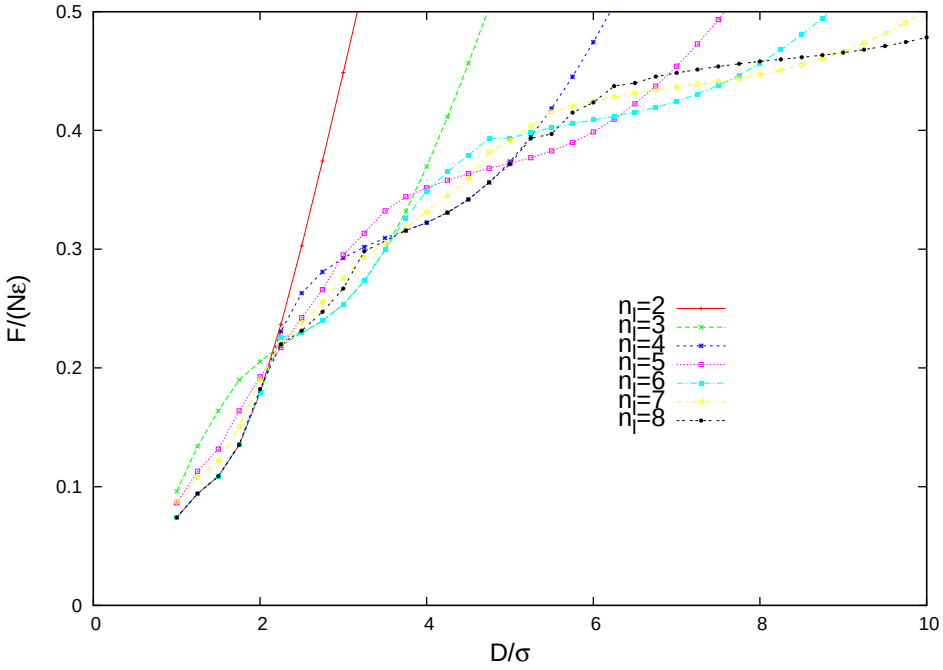

Figure 5.6.: $F/(N\epsilon)$ of a layered system at bulk density $\rho^* = 0.4$ vs. D/σ. Different curves correspond to different number of layers n_l(see inset).

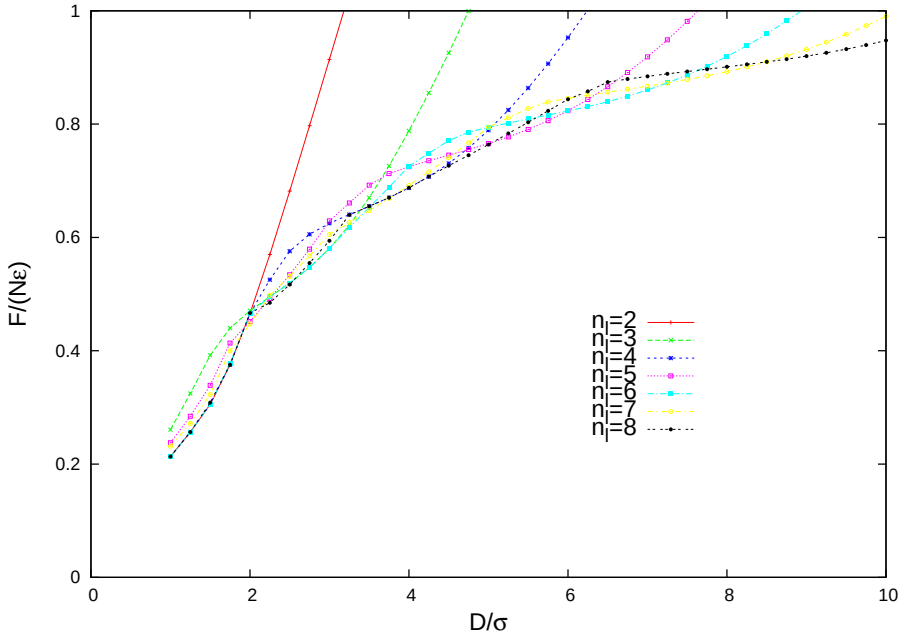

Figure 5.7.: $F/(N\epsilon)$ of a layered system at bulk density $\rho^* = 0.6$ vs. D/σ. Different curves correspond to different number of layers n_l(see inset).

5.3. Structures

This section cotains the details about the structures of the layered configurations described above.

In all systems, the layers were found to be equally spaced (within numerical accuracy) between the walls, $h_i = D/(n_l - 1)$.

The following tables provide the structural details. The explicit data sets are compiled in appendix B.

Structures at $\rho = 0.05$

D/σ	n_l	2-D structures	lattice parameter	(x, y) displacement	View into $< 1, 0, 0 >$
1.00	2	oblique	$a/\sigma = 8.53$ $b/\sigma = 4.76$ φ=1.40	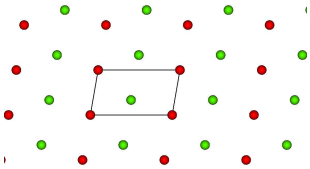	
2.00	2	rectangular	$a/\sigma = 5.09$ $b/\sigma = 3.93$	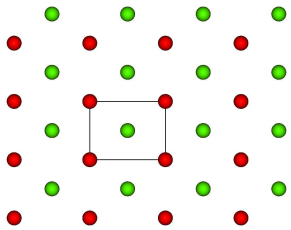	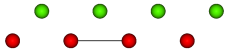
2.50	2	square	$a/\sigma = 4.00$	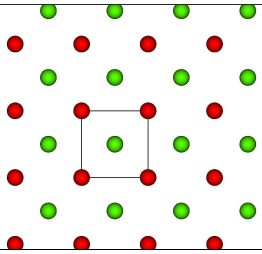	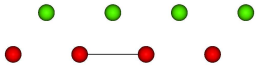
3.25	2	hexagonal	$a/\sigma = 3.77$	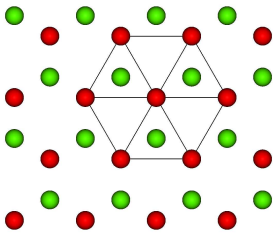	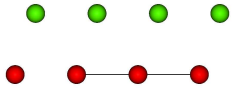

4.00	3	rectangular	$a/\sigma = 4.14$ b/σ=3.62	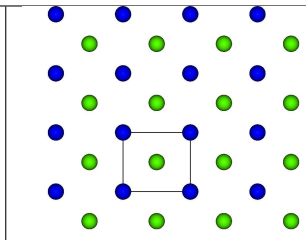	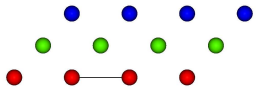
4.75	3	square	$a/\sigma = 3.55$	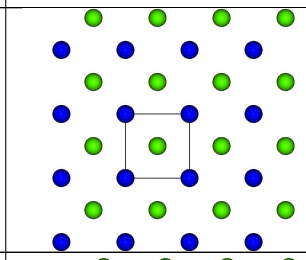	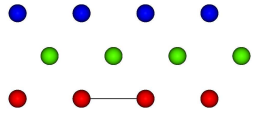
5.25	3	centered rectangular	$a/\sigma = 4.95$ $b/\sigma = 4.62$	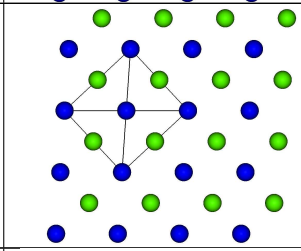	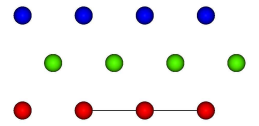
6.00	3	hexagonal	$a/\sigma = 3.40$	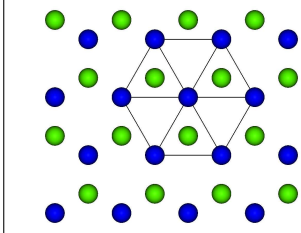	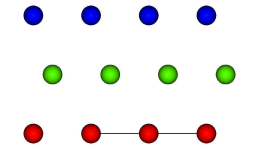
7.00	4	square	$a/\sigma = 3.38$	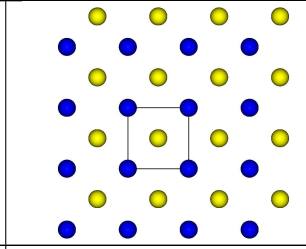	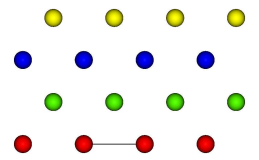
8.25	4	hexagonal	$a/\sigma = 3.35$	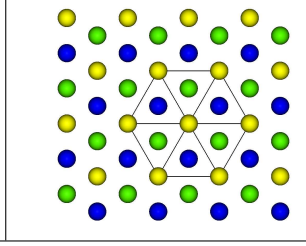	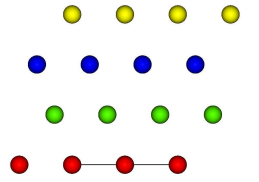

9.00	5	square	$a/\sigma = 3.33$	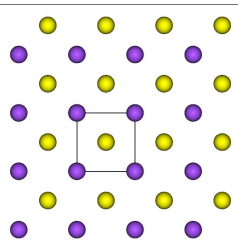	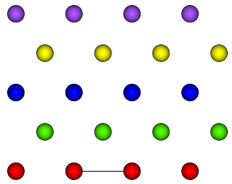
10.0	5	centered rectangular	$a/\sigma = 4.76$ $b/\sigma = 4.20$	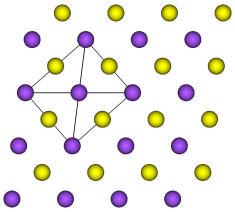	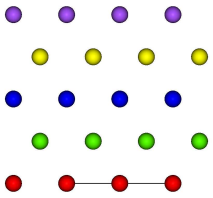

Table 5.1.: Structural details of the stable layered arrangements of a system with fixed bulk number density $\rho^* = 0.05$. Particles with the same color belong to the same layer.

Structures at $\rho^* = 0.1$

D/σ	n_l	2-D structures	lattice parameter	(x, y) displacement	View into $< 1, 0, 0 >$
1.00	2	rectangular	$a/\sigma = 5.68$ $b/\sigma = 3.52$	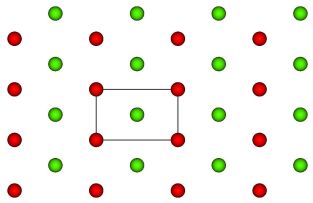	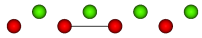
2.00	2	square	$a/\sigma = 3.16$	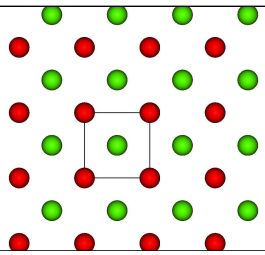	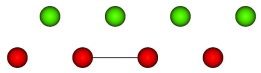
2.50	2	hexagonal	$a/\sigma = 3.04$	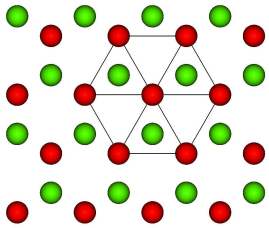	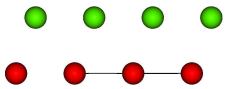
3.75	3	square	$a/\sigma = 2.83$	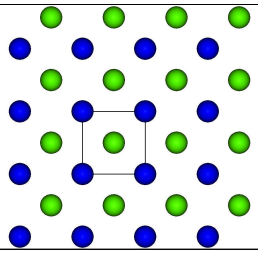	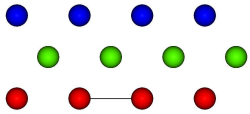
4.50	3	hexagonal	$a/\sigma = 2.77$	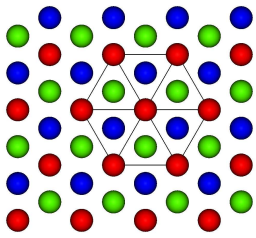	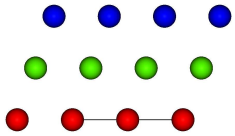
5.50	4	square	$a/\sigma = 2.70$	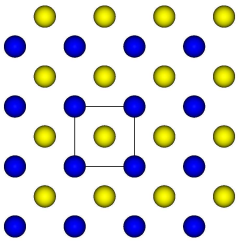	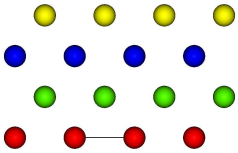

6.00	4	centered rectangular	$a/\sigma = 3.93$ $b/\sigma = 3.39$	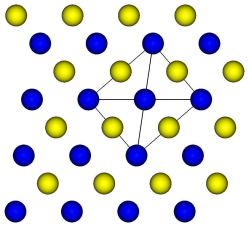	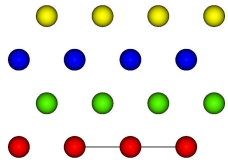
6.50	4	hexagonal	$a/\sigma = 2.67$	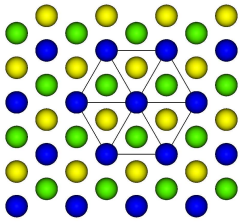	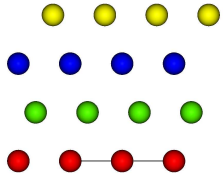
7.50	5	square	$a/\sigma = 2.58$	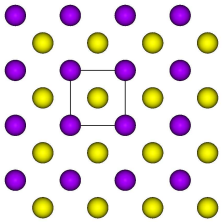	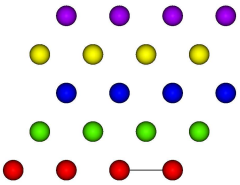
8.50	5	hexagonal	$a/\sigma = 2.61$	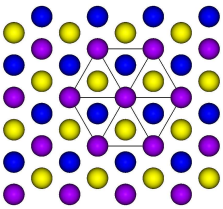	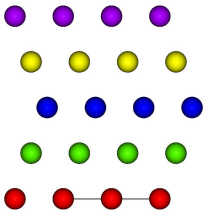

Table 5.2.: Structural details of the stable layered arrangements of a system with fixed bulk number density $\rho^* = 0.10$. Particles with the same color belong to the same layer.

Structure at $\rho^* = 0.2$

D/σ	n_l	2-D structures	lattice parameter	(x, y) displacement	View into $< 1, 0, 0 >$
1.00	2	rectangular	$a/\sigma = 3.79$ $b/\sigma = 2.64$	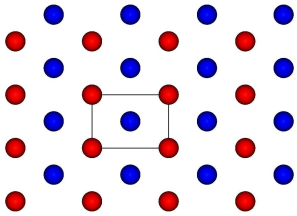	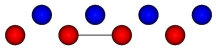
1.50	2	square	$a/\sigma = 2.58$	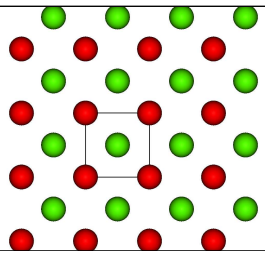	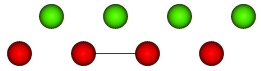
2.00	2	hexagonal	$a/\sigma = 2.40$	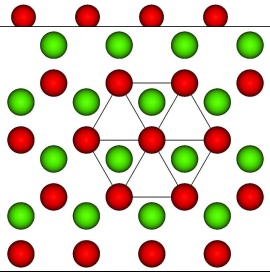	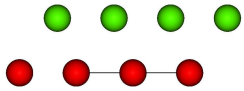
3.00	3	square	$a/\sigma = 2.24$	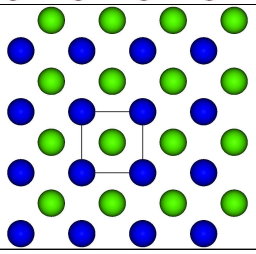	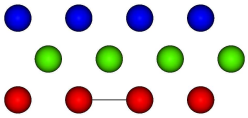
3.25	3	centered rectangular	$a/\sigma = 3.49$ $b/\sigma = 2.65$	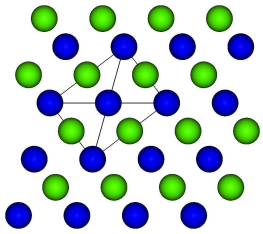	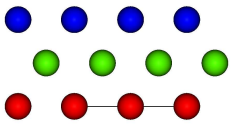
4.00	3	hexagonal	$a/\sigma = 2.08$	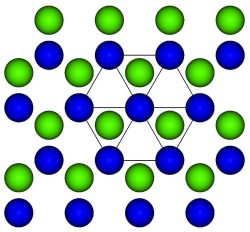	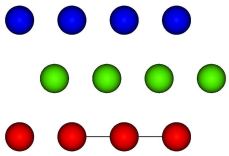

5.25	4	hexagonal	$a/\sigma = 2.10$	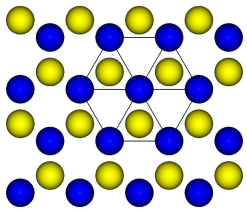	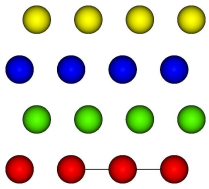
6.25	3	centered rectangular	$a/\sigma = 3.28$ $b/\sigma = 2.44$	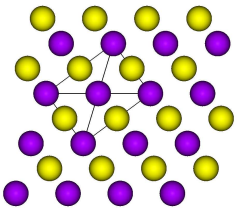	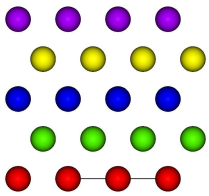

Table 5.3.: Structural details of the stable layered arrangements of a system with fixed bulk number density $\rho^* = 0.20$. Particles with the same color belong to the same layer.

Structures at $\rho^* = 0.4$

D/σ	n_l	2-D structures	lattice parameter	(x, y) displacement	View into $< 1, 0, 0 >$
1.25	2	square	$a/\sigma = 2.00$	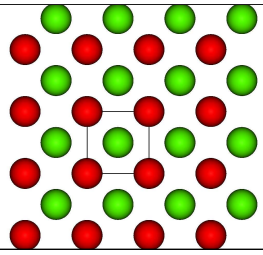	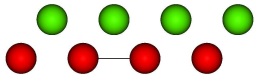
1.75	2	hexagonal	$a/\sigma = 1.82$	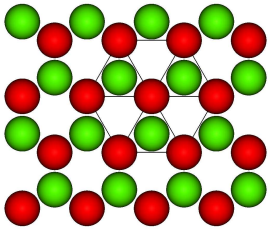	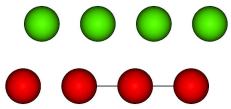
2.25	3	square	$a/\sigma = 1.83$	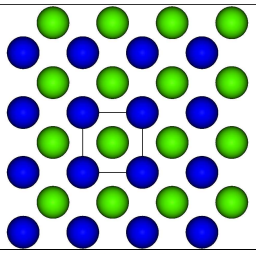	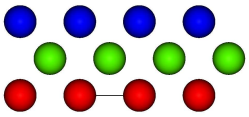
2.75	3	centered rectangular	$a/\sigma = 2.87$ $b/\sigma = 1.90$	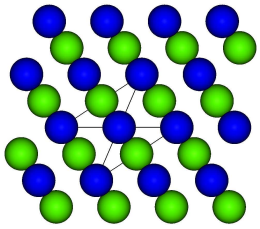	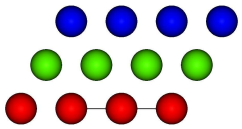
3.50	3	hexagonal	$a/\sigma = 1.57$	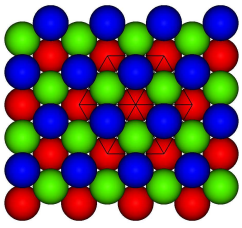	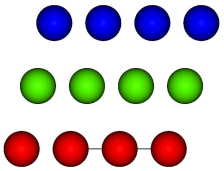
4.00	4	centered rectangular	$a/\sigma = 2.74$ $b/\sigma = 1.82$	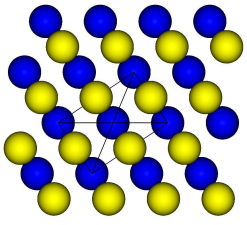	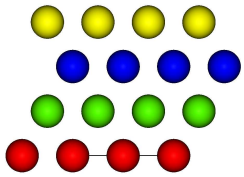

4.50	4	hexagonal	$a/\sigma = 1.60$	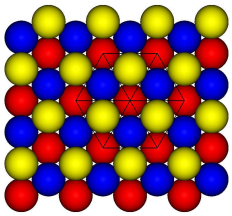	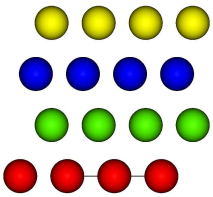

Table 5.4.: Structural details of the stable layered arrangements of a system with fixed bulk number density $\rho^* = 0.40$. Particles with the same color belong to the same layer.

Structures at $\rho^* = 0.6$

D/σ	n_l	2-D structures	lattice parameter	(x, y) displacement	View into $< 1, 0, 0 >$
1.00	2	square	$a/\sigma = 1.83$	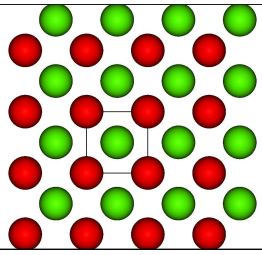	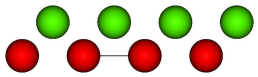
1.25	2	centered rectangular	$a/\sigma = 2.84$ $b/\sigma = 1.87$	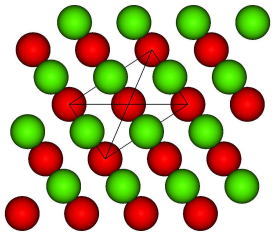	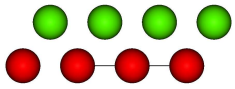
1.75	2	hexagonal	$a/\sigma = 1.48$	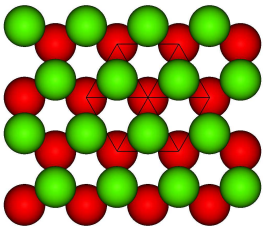	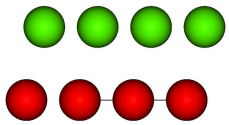
2.25	3	centered rectangular	$a/\sigma = 2.54$ $b/\sigma = 1.75$	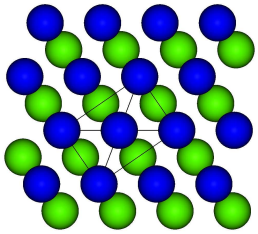	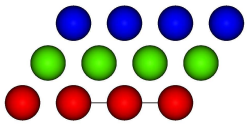
2.75	3	hexagonal	$a/\sigma = 1.45$	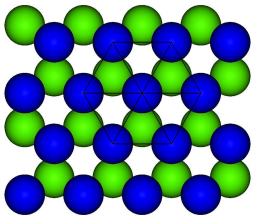	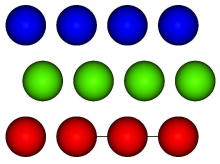

Table 5.5.: Structural details of the stable layered arrangements of a system with fixed bulk number density $\rho^* = 0.60$. Particles with the same color belong to the same layer.

5.4. Bulk limit

If we increase D further, we expect that the system will form its stable bulk crystal structure. In this thesis we have investigated this behaviour of the system at $\rho^* = 0.1$ and wall distances up to $D = 100\sigma$. The zero-temperature solid phase of the Gaussian core model of the bulk system, at $\rho^* = 0.1$ indicates a stable fcc phase with a free energy per particle of 0.0173.

5.4.1. fcc stacking

The fcc lattice can be built up by stacked two-dimensional Bravais lattices, via one of the following ways:

- **Square**: The two-dimensional lattice is a square lattice with a lattice parameter a. The stacking sequence is $ABAB\ldots$ in the $< 100 >$ direction. Each layer is displaced by $(a/2, a/2)$ in the (x, y)-plane. The vertical distance between the two layers is $a/\sqrt{2}$. The corresponding fcc lattice constant is a.
- **Rectangular**: The two-dimensional lattice is a rectangular lattice with lattice parameters a and b. The stacking sequence is $ABAB\ldots$ in the $< 11'0 >$ direction. Each layer is displaced by $(a/2, a/\sqrt{8})$ in the (x, y)-plane. The vertical distance between the two layers is $a/\sqrt{8}$. The corresponding fcc lattice constant is a.
- **Hexagonal**: The two-dimensional lattice is a hexagonal lattice with a lattice parameter a. The stacking sequence is $ABCABC\ldots$ in the $< 111 >$ direction. Each layer is displaced by $(a/2, a/\sqrt{12})$ in the (x, y)-plane. The vertical distance between two layers is $\sqrt{2/3}a$. The corresponding fcc lattice constant is $\sqrt{2}a$.

To identify the layered system, as an fcc crystal, the particle and layer arrangement has to fullfill the conditions of one of the three cases.

Structures and free energy

For the considered system, the free energy curves are depicted in figure 5.8.

We can see, that with increasing D and n_l, the free energies of the systems approach the free energy of the fcc bulk phase.

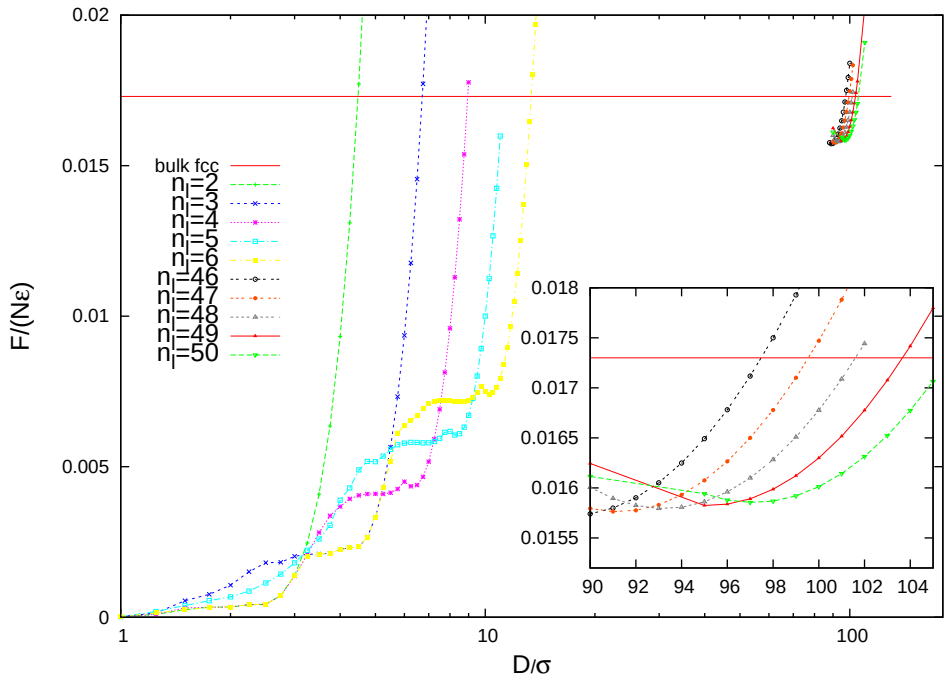

Figure 5.8.: $F/(N\epsilon)$ of a layered system with bulk density $\rho^* = 0.10$ vs. D/σ with an enlargement of the for the region with a large number of particles layers, i.e., $47 \leq n_l \leq 50$. Different curves correspond to different number of layers n_l. Note the different scales of D in the figure.

The stable two-dimensional structures for all the investigated configurations are hexagonal structures. The layers were found to be equally spaced between the walls, i.e., $h_i = D/(n_l - 1)$. Furthermore the layer distances fulfill the condition of $\sqrt{2/3}a$ for an fcc crystal, formed by stacked hexagonal layers. Therefore one can assume, that in the bulk limit the system will converge to an fcc crystal.

The layer displacement in the (x, y)-direction is of course not unique. We have found layer displacements of $(a/2, a/\sqrt{12})$ and $(a, \sqrt{3})$; both lead to the same fcc crystal structure. In our results we have seen, that squences of equal layer displacements appear in blocks with stacking pattern $ABCABC\ldots$. Due to competing structures these fcc-like blocks become $ABCBCABC\ldots$ at the boundaries, which might be similar to a mechanism like stacking faults. For all these cases, the displacement in z direction remains constant. The reference data can be found in appendix B.

In the following table the above results are summerized in detail.

D/σ	n_l	lattice parameter	2-D structure	layer distance	View into $< 0, 0, 1 >$	(x, y) displacement
94.0	48	$a/\sigma = 2.43$	hexagonal	d/a=0.82	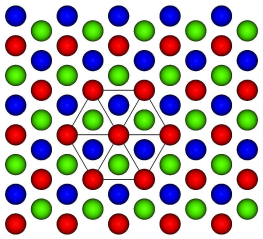	(1.21,0.70)
95.0	49	$a/\sigma = 2.44$	hexagonal	d/a=0.81	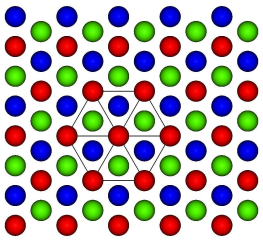	(1.22,0.70)
96.0	49	$a/\sigma = 2.43$	hexagonal	d/a=0.81	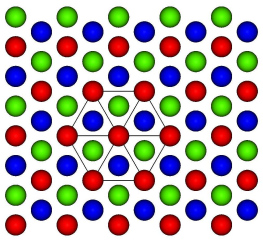	(2.43,1.40)
97.0	50	$a/\sigma = 2.44$	hexagonal	d/a= 0.82	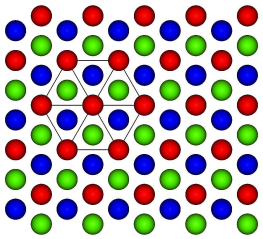	(1.22,0.71)

Table 5.6.: Structural details of the stable layered arrangements of a system with fixed bulk number density $\rho^* = 0.10$ for large wall distances D. The number of layers is denoted by n_l. Particles with the same color belong to the same layer.

5.4.2. Buckling

The transition region, where with increasing D the insertion of an additional layer is energetically more favourable, is not a sharp transition as the phase diagram in figure 5.2 might suggest. To viusalize this, we consider a density $\rho^* = 0.10$. In a region $2.5\sigma \leq D \leq 3.4\sigma$ a six layer arrangement guarantees a lower energy than the two layer arrangement or the three layer arrangement. Here the buckling transition mechanism comes into play, first identified by Pansu *et al.* [28], and the occurrence of prism phases for transitions with higher n_l, introduced by Bechinger *et al.* [29].

In this thesis we have investigated the layer transitions between two and three layers at $\rho^* = 0.10$. The calculations have been performed taking advantage that also coinciding layers can be treated within our algorithm, as introduced in section 5.2.

Layer transition $\mathbf{2n_l \longrightarrow 3n_l}$ at $\rho^* = 0.10$

The system is calculated with $n_l = 6$. At wall distance $D = 2.90\sigma$ the system forms two layers with a hexagonal structure and $eta = 0.145$. As the wall distance becomes $D = 3.00\sigma$. One sublayer with $\eta = 0.0483$, separates from the bottom layer and, similarly a sublayer with $\eta = 0.0483$ from the the top layer. At this step pyramids can be identified where the top particle are element of the newly formed layer, while rectangular bases are element of the top and the base layer. A further increase of D leads to an increase in the height of the pyramid. At $D = 3.30\sigma$ the system changes the structure instantaneously and forms three layers with square structure. A presumption is, that one of the pyramid's side surfaces, the triangle with the longer edge, provides a right angle and could therefore be a structural proposal, that forces the system to change instantaneously in the direction perpendicular to the triangle. Further investigations are necessary to clarify that.
The z component of the interlayer vector 1 and 5 are zero. The transition of the structure is shown in table 5.7. Further insight comes from the free energy as a function of wall distance. One clearly sees that the six-layer arrangement represents for a small D-range the energetic most favourable ordered structure, representing thereby the above described transition from a two- to a three-layer system. The reference data to this results is summerized in appendix A.

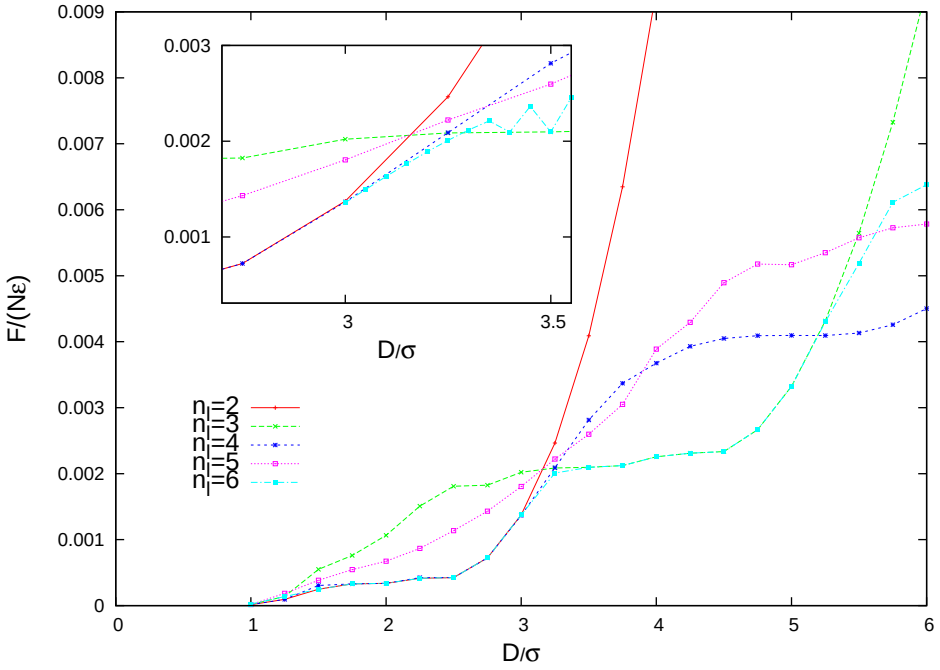

Figure 5.9.: $F/(N\epsilon)$ of a layered system with bulk density $\rho^* = 0.10$ vs. D/σ with an enlargement of the transition region between $n_l = 2$ and $n_l = 3$. Different curves correspond to different number of layers n_l (see inset

View into $< 0, 0, 1 >$	View into $< 1, 0, 0 >$
$D/\sigma = 2.90$	
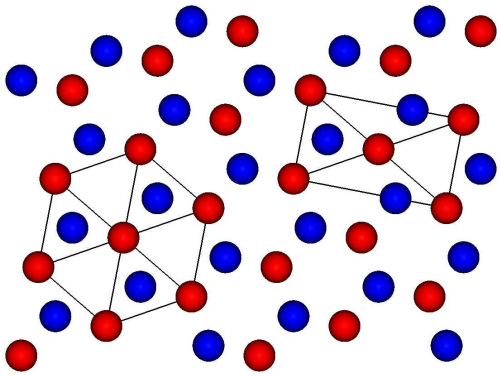	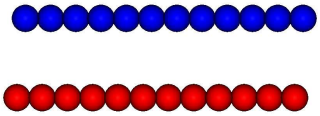
$D/\sigma = 3.00$	
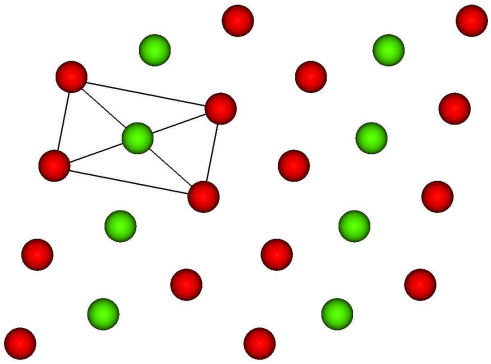	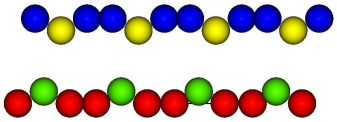
$D/\sigma = 3.10$	
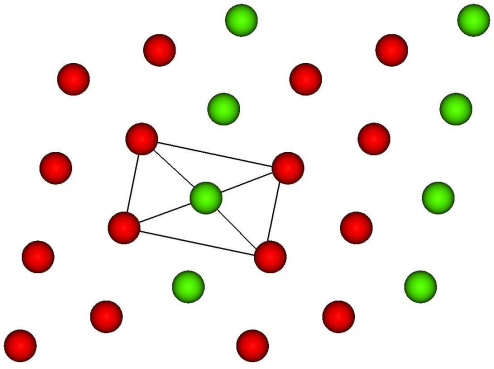	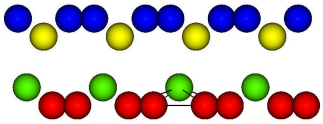
$D/\sigma = 3.20$	

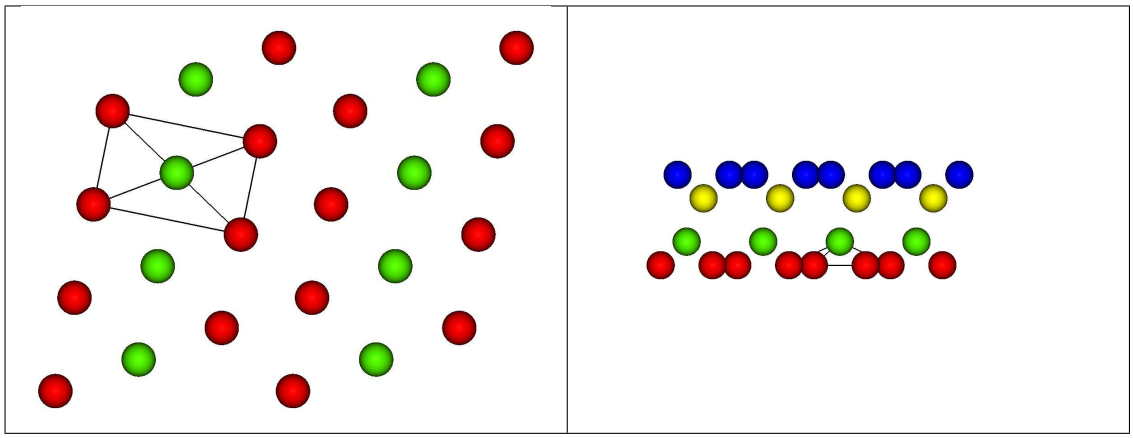

$D/\sigma = 3.25$

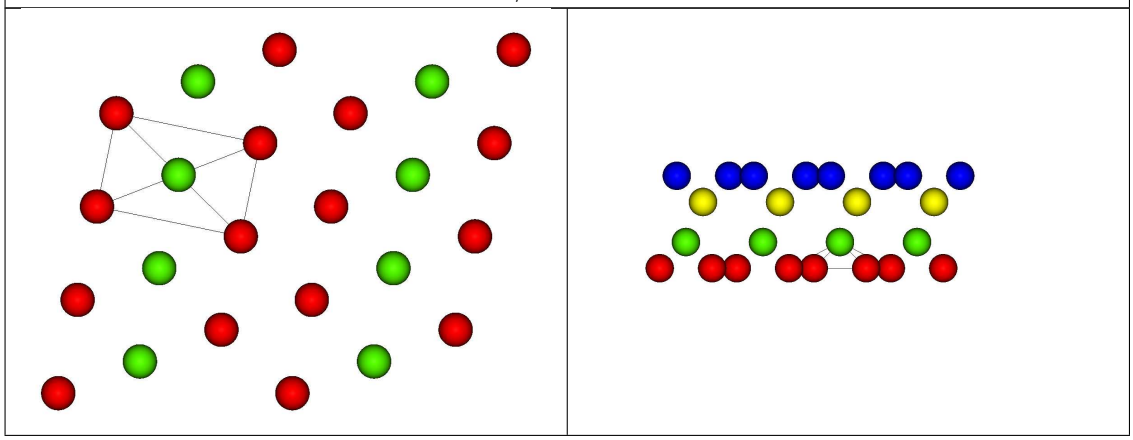

$D/\sigma = 3.27$

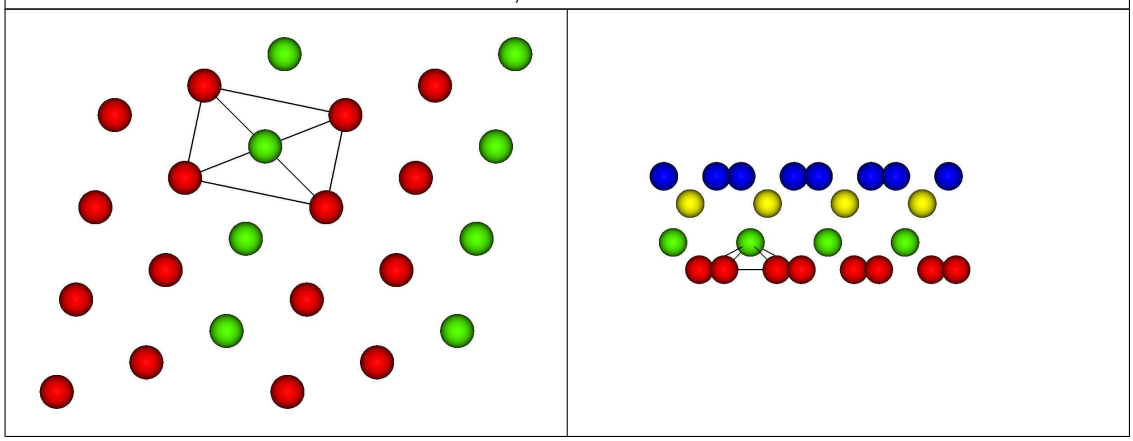

$D/\sigma = 3.30$

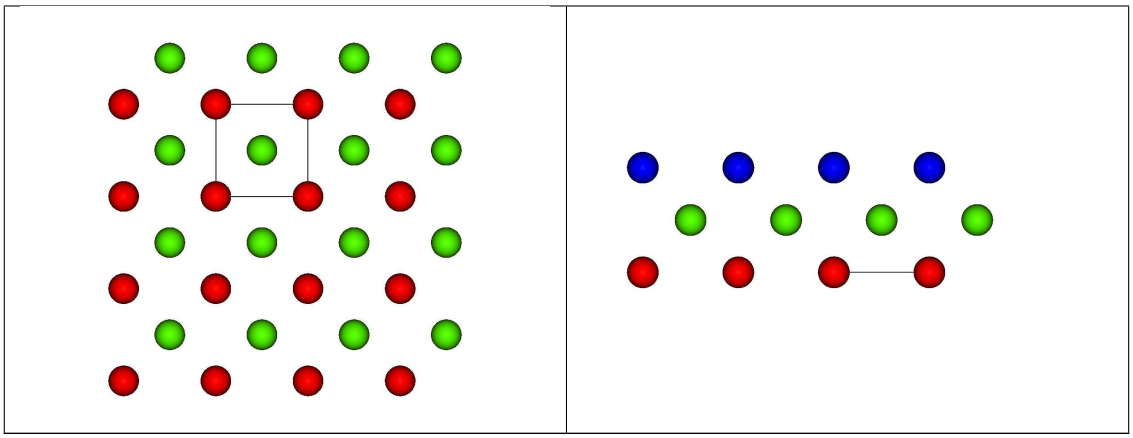

Table 5.7.: Structural details of the layer transition from $n_l = 2$ to $n_l = 3$, at a fixed bulk number density $\rho^* = 0.10$. Particles with the same color belong to the same layer.

6. Summary

In this thesis we have studied ordered equilibrium structures of Gaussian particles confined between two parallel horizontal walls and separated by a distance D. Ordered structures are formed as layers and we studied how the formation of the layers takes place; as D and the number density ρ^* varies. Working in the canonical ensemble we have identified the energetically most favourable particle arrangements, obtained by minimizing the free energy. To find these configurations we have used search strategies, that are based on ideas of genetic algorithms. Thus we were able to provide the full phase diagram in (D, ρ^*)-space: it allows to locate the transition lines between the emerging structures and the number of layers that the system forms. For small number densities $\rho^* \leq 0.1$ and for wall distances $D > 2\sigma$ we have found that morphological transitions can be identified described via the well known transition relation [50]

$$n_l\Delta \longrightarrow (n_l + 1)\square \longrightarrow (n_l + 1)\triangle, \tag{6.1}$$

where n_l is the the number of layers, $\square$ and $\triangle$ correspond to layers of quadratic and hexagonal symmetry. In addition, a rectangular region for $D < 2\sigma$ could be identified.
For large number densities, $\rho^* > 0.5$, we have identified a transition sequence, that can be symbolically described as:

$$2\square \longrightarrow 2r \longrightarrow 2\triangle \longrightarrow 3r \longrightarrow 3\triangle \longrightarrow 4r \longrightarrow 4\triangle \ldots \tag{6.2}$$

where $\square$, r, and $\triangle$ correspond to layers of quadratic, centered rectangular and hexagonal symmetry.

Furthermore, we have considered the limit of large wall distances, knowing that for $\rho = 0.1$ and large D-values the layered system will convert into a fcc stacked bulk crystall. Indeed, we obtain a layered stack, with hexagonal symmetry and layer distances of $a/\sqrt{8}$. The stacking sequence could be identified to have the form $ABCABC\ldots$.

Finally we provided a deeper insight into the transition mechanism from a two to a three-layered system at $\rho^* = 0.10$ as D slowly increases. Taking benefit of the fact that our approach also allows for coinciding layers we were able to investigate this problem and to depict a detailed sequence of figures with increasing D, that represent the structural behaviour during the transition. Thus a transition from a hexagonal lattice via a structure, similar to a pyramid, with an instantaneous change to a lattice with squared structure at the end, could be verified.

A. Numerical Details

Most of the GA calculations in this thesis were carried out with the following values for the parameters (for definitions carried from chapter 4)

Parameter	Value
l_{n}	12
l_{a}	6
p_{mutate}	0.35%
number of individuals n	500
number of populations	1200
δ_{thresh}	1×10^{-10}
r_{cut}	$\sim 4.3\sigma$

B. Reference Data

This chapter contains the referece data of the described configurations in this thesis.

B.1. Reference data of the described structures

```
wall distance=       1.00000000
rho=       0.05000000
minimal free energy =       0.00000000
name: 2D oblique, a=8.53076 b=4.75898 gamma=1.39899
number density:     0.050000
area density:     0.025000
 number of layers:            2
lattice vectors:
a:     8.530757    0.000000
b:     0.813604    4.688916
inter-layer vectors
  1    4.242852    1.562590    1.000000
-----------------------------------------------
wall distance=       2.00000000
rho=       0.05000000
minimal free energy =       0.00000138
name: 2D rectangular, a=5.09402 b=3.92617
number density:     0.050000
area density:     0.050000
 number of layers:            2
lattice vectors:
a:     5.094022    0.000000
b:     0.000000    3.926170
inter-layer vectors
  1    2.547011    1.963085    2.000000
-----------------------------------------------
wall distance=       2.50000000
rho=       0.05000000
minimal free energy =       0.00000152
name: 2D square, a=4.00000
number density:     0.050000
area density:     0.062500
 number of layers:            2
lattice vectors:
a:     4.000000    0.000000
b:     0.000000    4.000000
inter-layer vectors
  1    2.000000    2.000000    2.500000
-----------------------------------------------
wall distance=       3.25000000
rho=       0.05000000
minimal free energy =       0.00000236
name: 2D hexagonal, a=3.76984
number density:     0.050000
area density:     0.081250
 number of layers:            2
lattice vectors:
a:     3.769841    0.000000
b:     1.884920    3.264778
inter-layer vectors
  1    1.884920    1.088259    3.250000
-----------------------------------------------
wall distance=       4.00000000
rho=       0.05000000
minimal free energy =       0.00002733
name: 2D rectangular, a=4.13794 b=3.62499
number density:     0.050000
area density:     0.066667
 number of layers:            3
lattice vectors:
a:     4.137940    0.000000
b:     0.000000    3.624993
inter-layer vectors
  1    2.068970    1.812496    2.000000
  2    2.068970    1.812496    2.000000
-----------------------------------------------
wall distance=       4.75000000
rho=       0.05000000
minimal free energy =       0.00002365
name: 2D square, a=3.55409
number density:     0.050000
area density:     0.079167
 number of layers:            3
lattice vectors:
a:     3.554093    0.000000
b:     0.000000    3.554093
inter-layer vectors
  1    1.777047    1.777047    2.375000
  2    1.777047    1.777047    2.375000
-----------------------------------------------
wall distance=       5.25000000
rho=       0.05000000
minimal free energy =       0.00003070
name: 2D centered rectangular, a=4.94825 b=4.61923
number density:     0.050000
area density:     0.087500
 number of layers:            3
lattice vectors:
a:     3.384617    0.000000
b:     0.232514    3.376621
inter-layer vectors
  1    1.808566    1.688311    2.625000
  2    1.808566    1.688311    2.625000
-----------------------------------------------
wall distance=       6.00000000
rho=       0.05000000
minimal free energy =       0.00003425
name: 2D hexagonal, a=3.39809
number density:     0.050000
area density:     0.100000
 number of layers:            3
lattice vectors:
a:     3.398089    0.000000
b:     1.699044    2.942831
inter-layer vectors
  1    1.699044    0.980944    3.000000
  2    3.398089    1.961887    3.000000
```

```
------------------------------------------------
wall distance=       7.00000000
rho=       0.05000000
minimal free energy =       0.00006451
name: 2D square, a=3.38062
number density:     0.050000
area density:     0.087500
 number of layers:            4
lattice vectors:
a:     3.380617    0.000000
b:     0.000000    3.380617
inter-layer vectors
  1    1.690308    1.690309    2.333333
  2    1.690308    1.690308    2.333333
  3    1.690308    1.690309    2.333333
------------------------------------------------
wall distance=       8.25000000
rho=       0.05000000
minimal free energy =       0.00006912
name: 2D hexagonal, a=3.34621
number density:     0.050000
area density:     0.103125
 number of layers:            4
lattice vectors:
a:     3.346206    0.000000
b:     1.673103    2.897900
inter-layer vectors
  1    3.346206    1.931933    2.750000
  2    3.346206    1.931933    2.750000
  3    3.346206    1.931933    2.750000
------------------------------------------------
wall distance=       9.00000000
rho=       0.05000000
minimal free energy =       0.00010820
name: 2D square, a=3.33333
number density:     0.050000
area density:     0.090000
 number of layers:            5
lattice vectors:
a:     3.333333    0.000000
b:     0.000000    3.333333
inter-layer vectors
  1    1.666667    1.666667    2.250000
  2    1.666667    1.666667    2.250000
  3    1.666667    1.666667    2.250000
  4    1.666667    1.666667    2.250000
------------------------------------------------
wall distance=      10.00000000
rho=       0.05000000
minimal free energy =       0.00013213
name: 2D centered rectangular, a=4.76386 b=4.19828
number density:     0.050000
area density:     0.100000
 number of layers:            5
lattice vectors:
a:     3.174897    0.000000
b:     0.399136    3.149708
inter-layer vectors
  1    1.787016    1.574854    2.500000
  2    1.787016    1.574854    2.500000
  3    1.787016    1.574854    2.500000
  4    1.787016    1.574854    2.500000
------------------------------------------------
wall distance=       1.00000000
rho=       0.10000000
minimal free energy =       0.00001454
name: 2D rectangular, a=5.68228 b=3.51971
number density:     0.100000
area density:     0.050000
 number of layers:            2
lattice vectors:
a:     5.682284    0.000000
b:     0.000000    3.519711
inter-layer vectors
  1    2.841142    1.759856    1.000000
------------------------------------------------
wall distance=       2.00000000
rho=       0.10000000
minimal free energy =       0.00033762
name: 2D square, a=3.16228
number density:     0.100000
area density:     0.100000
 number of layers:            2
lattice vectors:
a:     3.162278    0.000000
b:     0.000000    3.162278
inter-layer vectors
  1    1.581139    1.581139    2.000000
------------------------------------------------
wall distance=       2.50000000
rho=       0.10000000
minimal free energy =       0.00042513
name: 2D hexagonal, a=3.03934
number density:     0.100000
area density:     0.125000
 number of layers:            2
lattice vectors:
a:     3.039343    0.000000
b:     1.519671    2.632148
inter-layer vectors
  1    1.519671    0.877383    2.500000
------------------------------------------------
wall distance=       3.75000000
rho=       0.10000000
minimal free energy =       0.00212344
name: 2D square, a=2.82843
number density:     0.100000
area density:     0.125000
 number of layers:            3
lattice vectors:
a:     2.828427    0.000000
b:     0.000000    2.828427
inter-layer vectors
  1    1.414214    1.414214    1.875000
  2    1.414214    1.414214    1.875000
------------------------------------------------
wall distance=       4.50000000
rho=       0.10000000
minimal free energy =       0.00233442
name: 2D hexagonal, a=2.77453
number density:     0.100000
area density:     0.150000
 number of layers:            3
lattice vectors:
a:     2.774528    0.000000
b:     1.387264    2.402811
inter-layer vectors
  1    1.387264    0.800937    2.250000
  2    1.387264    0.800937    2.250000
------------------------------------------------
wall distance=       5.50000000
rho=       0.10000000
minimal free energy =       0.00413268
name: 2D square, a=2.69680
number density:     0.100000
area density:     0.137500
 number of layers:            4
lattice vectors:
a:     2.696799    0.000000
b:     0.000000    2.696799
inter-layer vectors
  1    1.348400    1.348400    1.833249
  2    1.348400    1.348400    1.833503
  3    1.348400    1.348400    1.833249
------------------------------------------------
wall distance=       6.00000000
rho=       0.10000000
minimal free energy =       0.00450234
name: 2D centered rectangular, a=3.93039 b=3.39237
number density:     0.100000
```

```
area density:     0.150000
 number of layers:            4
lattice vectors:
a:     2.595965    0.000000
b:     0.379415    2.568088
inter-layer vectors
  1    1.487690    1.284044    1.999992
  2    1.487690    1.284044    2.000015
  3    1.487690    1.284044    1.999992
-----------------------------------------------
wall distance=       6.50000000
rho=       0.10000000
minimal free energy =       0.00438880
name: 2D hexagonal, a=2.66568
number density:     0.100000
area density:     0.162500
 number of layers:            4
lattice vectors:
a:     2.665680    0.000000
b:     1.332840    2.308547
inter-layer vectors
  1    1.332840    0.769516    2.166667
  2    2.665680    1.539031    2.166667
  3    2.665680    1.539031    2.166666
-----------------------------------------------
wall distance=       7.50000000
rho=       0.10000000
minimal free energy =       0.00594277
name: 2D square, a=2.58199
number density:     0.100000
area density:     0.150000
 number of layers:            5
lattice vectors:
a:     2.581989    0.000000
b:     0.000000    2.581989
inter-layer vectors
  1    1.290994    1.290994    1.874943
  2    1.290994    1.290994    1.875057
  3    1.290994    1.290994    1.875057
  4    1.290994    1.290994    1.874943
-----------------------------------------------
wall distance=       8.50000000
rho=       0.10000000
minimal free energy =       0.00609779
name: 2D hexagonal, a=2.60621
number density:     0.100000
area density:     0.170000
 number of layers:            5
lattice vectors:
a:     2.606215    0.000000
b:     1.303107    2.257048
inter-layer vectors
  1    1.303107    0.752349    2.124999
  2    1.303107    0.752349    2.125001
  3    2.606215    1.504699    2.125001
  4    2.606215    1.504699    2.124999
-----------------------------------------------
wall distance=       1.00000000
rho=       0.20000000
minimal free energy =       0.00450678
name: 2D rectangular, a=3.78992 b=2.63858
number density:     0.200000
area density:     0.100000
 number of layers:            2
lattice vectors:
a:     3.789920    0.000000
b:     0.000000    2.638578
inter-layer vectors
  1    1.894960    1.319289    1.000000
-----------------------------------------------
wall distance=       1.50000000
rho=       0.20000000
minimal free energy =       0.01006855
name: 2D square, a=2.58199
number density:     0.200000
area density:     0.150000
 number of layers:            2
lattice vectors:
a:     2.581989    0.000000
b:     0.000000    2.581989
inter-layer vectors
  1    1.290994    1.290994    1.500000
-----------------------------------------------
wall distance=       2.00000000
rho=       0.20000000
minimal free energy =       0.01334889
name: 2D hexagonal, a=2.40281
number density:     0.200000
area density:     0.200000
 number of layers:            2
lattice vectors:
a:     2.402811    0.000000
b:     1.201406    2.080896
inter-layer vectors
  1    2.402811    1.387264    2.000000
-----------------------------------------------
wall distance=       2.75000000
rho=       0.20000000
minimal free energy =       0.03509677
name: 2D square, a=2.33550
number density:     0.200000
area density:     0.183333
 number of layers:            3
lattice vectors:
a:     2.335497    0.000000
b:     0.000000    2.335497
inter-layer vectors
  1    1.167748    1.167748    1.375000
  2    1.167748    1.167748    1.375000
-----------------------------------------------
wall distance=       3.00000000
rho=       0.20000000
minimal free energy =       0.03668223
name: 2D square, a=2.23607
number density:     0.200000
area density:     0.200000
 number of layers:            3
lattice vectors:
a:     2.236068    0.000000
b:     0.000000    2.236068
inter-layer vectors
  1    1.118034    1.118034    1.500000
  2    1.118034    1.118034    1.500000
-----------------------------------------------
wall distance=       4.00000000
rho=       0.20000000
minimal free energy =       0.04827120
name: 2D hexagonal, a=2.08090
number density:     0.200000
area density:     0.266667
 number of layers:            3
lattice vectors:
a:     2.080896    0.000000
b:     1.040448    1.802109
inter-layer vectors
  1    2.080896    1.201406    2.000000
  2    1.040448    0.600703    2.000000
-----------------------------------------------
wall distance=       5.25000000
rho=       0.20000000
minimal free energy =       0.06147409
name: 2D hexagonal, a=2.09735
number density:     0.200000
area density:     0.262500
 number of layers:            4
lattice vectors:
a:     2.097346    0.000000
b:     1.048673    1.816355
inter-layer vectors
  1    1.048673    0.605452    1.749964
```

```
  2    2.097346    1.210903    1.750071
  3    1.048673    0.605452    1.749964
-----------------------------------------------
wall distance=       6.25000000
rho=       0.20000000
minimal free energy =       0.07434312
name: 2D centered rectangular, a=3.28246 b=2.43719
number density:     0.200000
area density:     0.250000
 number of layers:            5
lattice vectors:
a:     2.044167    0.000000
b:     0.591273    1.956787
inter-layer vectors
  1    1.317720    0.978394    1.562022
  2    1.317720    0.978394    1.562978
  3    1.317720    0.978394    1.562978
  4    1.317720    0.978393    1.562022
-----------------------------------------------
wall distance=       1.25000000
rho=       0.40000000
minimal free energy =       0.09407613
name: 2D square, a=2.00000
number density:     0.400000
area density:     0.250000
 number of layers:            2
lattice vectors:
a:     2.000000    0.000000
b:     0.000000    2.000000
inter-layer vectors
  1    1.000000    1.000000    1.250000
-----------------------------------------------
wall distance=       1.75000000
rho=       0.40000000
minimal free energy =       0.13518630
name: 2D hexagonal, a=1.81635
number density:     0.400000
area density:     0.350000
 number of layers:            2
lattice vectors:
a:     1.816355    0.000000
b:     0.908177    1.573009
inter-layer vectors
  1    0.908177    0.524336    1.750000
-----------------------------------------------
wall distance=       2.25000000
rho=       0.40000000
minimal free energy =       0.21874645
name: 2D square, a=1.82574
number density:     0.400000
area density:     0.300000
 number of layers:            3
lattice vectors:
a:     1.825742    0.000000
b:     0.000000    1.825742
inter-layer vectors
  1    0.912871    0.912871    1.125000
  2    0.912871    0.912871    1.125000
-----------------------------------------------
wall distance=       2.75000000
rho=       0.40000000
minimal free energy =       0.23973816
name: 2D centered rectangular, a=2.87649 b=1.89625
number density:     0.400000
area density:     0.366667
 number of layers:            3
lattice vectors:
a:     1.722641    0.000000
b:     0.678965    1.583193
inter-layer vectors
  1    1.200804    0.791596    1.375000
  2    1.200803    0.791596    1.375000
-----------------------------------------------
wall distance=       3.50000000
rho=       0.40000000
minimal free energy =       0.29963718
name: 2D hexagonal, a=1.57301
number density:     0.400000
area density:     0.466667
 number of layers:            3
lattice vectors:
a:     1.573009    0.000000
b:     0.786505    1.362266
inter-layer vectors
  1    0.786505    0.454089    1.750000
  2    0.786505    0.454089    1.750000
-----------------------------------------------
wall distance=       4.00000000
rho=       0.40000000
minimal free energy =       0.32237138
name: 2D centered rectangular, a=2.73945 b=1.82519
number density:     0.400000
area density:     0.400000
 number of layers:            4
lattice vectors:
a:     1.645894    0.000000
b:     0.633890    1.518931
inter-layer vectors
  1    1.139892    0.759465    1.331475
  2    1.139892    0.759465    1.337050
  3    1.139892    0.759466    1.331475
-----------------------------------------------
wall distance=       4.50000000
rho=       0.40000000
minimal free energy =       0.34184728
name: 2D hexagonal, a=1.60187
number density:     0.400000
area density:     0.450000
 number of layers:            4
lattice vectors:
a:     1.601874    0.000000
b:     0.800937    1.387264
inter-layer vectors
  1    1.601874    0.924843    1.499630
  2    1.601874    0.924843    1.500686
  3    0.800937    0.462421    1.499684
-----------------------------------------------
wall distance=       1.00000000
rho=       0.60000000
minimal free energy =       0.21321756
name: 2D square, a=1.82574
number density:     0.600000
area density:     0.300000
 number of layers:            2
lattice vectors:
a:     1.825742    0.000000
b:     0.000000    1.825742
inter-layer vectors
  1    0.912871    0.912871    1.000000
-----------------------------------------------
wall distance=       1.25000000
rho=       0.60000000
minimal free energy =       0.25656791
name: 2D centered rectangular, a=2.84478 b=1.87478
number density:     0.600000
area density:     0.375000
 number of layers:            2
lattice vectors:
a:     1.703495    0.000000
b:     0.671853    1.565409
inter-layer vectors
  1    1.187674    0.782705    1.250000
-----------------------------------------------
wall distance=       1.75000000
rho=       0.60000000
minimal free energy =       0.37542024
name: 2D hexagonal, a=1.48305
number density:     0.600000
area density:     0.525000
 number of layers:            2
```

```
lattice vectors:
a:      1.483047    0.000000
b:      0.741524    1.284357
inter-layer vectors
  1     0.741524    0.428119    1.750000
-----------------------------------------------
wall distance=       2.25000000
rho=       0.60000000
minimal free energy =       0.49529192
name: 2D centered rectangular, a=2.53673 b=1.75204
number density:     0.600000
area density:     0.450000
 number of layers:            3
lattice vectors:
a:      1.541479    0.000000
b:      0.545801    1.441617
inter-layer vectors
  1     1.043640    0.720808    1.125000
  2     1.043640    0.720808    1.125000
-----------------------------------------------
wall distance=       2.75000000
rho=       0.60000000
minimal free energy =       0.54699284
name: 2D hexagonal, a=1.44895
number density:     0.600000
area density:     0.550000
 number of layers:            3
lattice vectors:
a:      1.448950    0.000000
b:      0.724475    1.254827
inter-layer vectors
  1     0.724475    0.418276    1.375000
  2     1.448950    0.836551    1.375000
```

B.2. Reference data of the bulk limit section

```
wall distance=      94.00000000
rho=       0.10000000
minimal free energy =       0.01580673
name: 2D hexagonal, a=2.42824
number density:     0.100000
area density:     0.195833
 number of layers:           48
lattice vectors:
a:     2.428239    0.000000
b:     1.214119    2.102916
inter-layer vectors
  1    2.428239    1.401944    1.999993
  2    2.428239    1.401944    1.999996
  3    2.428239    1.401944    1.999996
  4    2.428239    1.401944    2.000001
  5    1.214119    0.700972    2.000001
  6    1.214119    0.700972    2.000001
  7    2.428239    1.401944    2.000006
  8    1.214119    0.700972    2.000006
  9    2.428239    1.401944    2.000006
 10    1.214119    0.700972    2.000001
 11    1.214119    0.700972    1.999996
 12    1.214119    0.700972    1.999996
 13    1.214119    0.700972    2.000001
 14    2.428239    1.401944    2.000006
 15    1.214119    0.700972    2.000001
 16    1.214119    0.700972    1.999996
 17    1.214119    0.700972    1.999996
 18    1.214119    0.700972    1.999996
 19    1.214119    0.700972    2.000001
 20    2.428239    1.401944    2.000001
 21    2.428239    1.401944    1.999996
 22    2.428239    1.401944    1.999996
 23    2.428239    1.401944    1.999996
 24    2.428239    1.401944    1.999996
 25    2.428239    1.401944    1.999996
 26    2.428239    1.401944    1.999996
 27    2.428239    1.401944    1.999996
 28    2.428239    1.401944    1.999996
 29    2.428239    1.401944    2.000001
 30    1.214119    0.700972    2.000006
 31    2.428239    1.401944    2.000001
 32    2.428239    1.401944    2.000001
 33    1.214119    0.700972    2.000006
 34    2.428239    1.401944    2.000006
 35    1.214119    0.700972    2.000006
 36    2.428239    1.401944    2.000001
 37    2.428239    1.401944    2.000001
 38    1.214119    0.700972    2.000006
 39    2.428239    1.401944    2.000001
 40    2.428239    1.401944    1.999996
 41    2.428239    1.401944    2.000001
 42    1.214119    0.700972    2.000001
 43    1.214119    0.700972    2.000001
 44    2.428239    1.401944    2.000006
 45    1.214119    0.700972    2.000001
 46    1.214119    0.700972    1.999996
 47    1.214119    0.700972    1.999993
-----------------------------------------------
wall distance=      95.00000000
rho=       0.10000000
minimal free energy =       0.01582471
name: 2D hexagonal, a=2.44046
number density:     0.100000
area density:     0.193878
 number of layers:           49
lattice vectors:
a:     2.440456    0.000000
b:     1.220228    2.113496
inter-layer vectors
  1    1.220228    0.704499    1.979156
  2    1.220228    0.704499    1.979167
  3    2.440456    1.408998    1.979174
  4    1.220228    0.704499    1.979168
  5    1.220228    0.704499    1.979161
  6    1.220228    0.704499    1.979167
  7    2.440456    1.408998    1.979168
  8    2.440456    1.408998    1.979167
  9    1.220228    0.704499    1.979167
 10    1.220228    0.704499    1.979167
 11    2.440456    1.408998    1.979174
 12    1.220228    0.704499    1.979174
 13    2.440456    1.408998    1.979167
 14    2.440456    1.408998    1.979167
 15    1.220228    0.704499    1.979174
 16    2.440456    1.408998    1.979174
 17    1.220228    0.704499    1.979167
 18    1.220228    0.704499    1.979161
 19    1.220228    0.704499    1.979161
 20    1.220228    0.704499    1.979161
 21    1.220228    0.704499    1.979161
 22    1.220228    0.704499    1.979161
 23    1.220228    0.704499    1.979161
 24    1.220228    0.704499    1.979168
 25    2.440456    1.408998    1.979174
 26    1.220228    0.704499    1.979174
 27    2.440456    1.408998    1.979167
 28    2.440456    1.408998    1.979167
 29    1.220228    0.704498    1.979174
 30    2.440456    1.408998    1.979168
 31    2.440456    1.408998    1.979161
 32    2.440456    1.408998    1.979161
 33    2.440456    1.408998    1.979167
 34    1.220228    0.704499    1.979167
 35    1.220228    0.704499    1.979161
 36    1.220228    0.704499    1.979167
 37    2.440456    1.408998    1.979174
 38    1.220228    0.704499    1.979174
 39    2.440456    1.408998    1.979167
 40    2.440455    1.408998    1.979161
 41    2.440456    1.408998    1.979161
 42    2.440456    1.408998    1.979167
 43    1.220228    0.704499    1.979174
 44    2.440456    1.408998    1.979167
 45    2.440456    1.408998    1.979167
 46    1.220228    0.704499    1.979167
 47    1.220228    0.704499    1.979161
 48    1.220228    0.704499    1.979156
-----------------------------------------------
wall distance=      96.00000000
rho=       0.10000000
minimal free energy =       0.01583766
name: 2D hexagonal, a=2.42771
number density:     0.100000
area density:     0.195918
 number of layers:           49
lattice vectors:
a:     2.427712    0.000000
b:     1.213856    2.102460
inter-layer vectors
  1    2.427712    1.401640    1.999993
  2    2.427712    1.401640    1.999996
  3    2.427712    1.401640    2.000001
  4    1.213856    0.700820    2.000001
  5    1.213856    0.700820    1.999996
  6    1.213856    0.700820    1.999996
  7    1.213856    0.700820    1.999996
  8    1.213856    0.700820    2.000001
  9    2.427712    1.401640    2.000001
 10    2.427712    1.401640    1.999996
 11    2.427712    1.401640    2.000001
 12    1.213856    0.700820    2.000006
 13    2.427712    1.401640    2.000006
 14    1.213856    0.700820    2.000006
```

```
 15    2.427712    1.401640    2.000006
 16    1.213856    0.700820    2.000006
 17    2.427712    1.401640    2.000001
 18    0.000000    1.401640    1.999996
 19    2.427712    1.401640    2.000001
 20    1.213856    0.700820    2.000001
 21    1.213856    0.700820    1.999996
 22    1.213856    0.700820    1.999996
 23    1.213856    0.700820    1.999996
 24    1.213856    0.700820    1.999996
 25    1.213856    0.700820    1.999996
 26    1.213856    0.700820    2.000001
 27    2.427712    1.401640    2.000006
 28    1.213856    0.700820    2.000001
 29    1.213856    0.700820    2.000001
 30    2.427712    1.401640    2.000001
 31    2.427712    1.401640    2.000001
 32    1.213856    0.700820    2.000001
 33    1.213856    0.700820    1.999996
 34    1.213856    0.700820    2.000001
 35    2.427712    1.401640    2.000006
 36    1.213856    0.700820    2.000001
 37    1.213856    0.700820    1.999996
 38    1.213856    0.700820    2.000001
 39    2.427712    1.401640    2.000001
 40    2.427712    1.401640    2.000001
 41    1.213856    0.700820    2.000001
 42    1.213856    0.700820    2.000001
 43    2.427712    1.401640    2.000001
 44    2.427711    1.401640    1.999996
 45    2.427712    1.401640    2.000001
 46    1.213856    0.700820    2.000006
 47    2.427711    1.401640    2.000001
 48    2.427712    1.401640    1.999993
-----------------------------------------------
wall distance=      97.00000000
rho=       0.10000000
minimal free energy =       0.01585455
name: 2D hexagonal, a=2.43969
number density:     0.100000
area density:     0.194000
 number of layers:           50
lattice vectors:
a:     2.439140    0.000000
b:     1.219993    2.113302
inter-layer vectors
  1    2.440238    1.406919    1.974347
  2    2.440513    1.407027    1.984857
  3    2.440609    1.407091    1.976208
  4    2.440543    1.406759    1.984188
  5    2.440256    1.407002    1.986331
  6    2.440363    1.406779    1.974328
  7    1.218730    0.706364    1.984475
  8    1.218800    0.706332    1.986069
  9    1.218726    0.706536    1.979225
 10    2.440359    1.406976    1.979154
 11    2.440337    1.406861    1.980165
 12    1.218903    0.706243    1.975839
 13    1.218594    0.706689    1.984635
 14    2.440539    1.406970    1.986044
 15    1.218631    0.706370    1.980162
 16    2.440352    1.407014    1.980133
 17    2.440326    1.407110    1.973822
 18    1.218678    0.706542    1.979254
 19    2.440348    1.406893    1.981192
 20    1.218502    0.706338    1.973582
 21    1.220407   -0.706396    1.978385
 22    2.440561    1.407033    1.981515
 23    1.218425    0.706256    1.982819
 24    2.438476    2.819698    1.981978
 25    1.218745    0.706593    1.981530
 26    1.218796    0.706224    1.981889
 27    2.440635    1.406830    1.980655
 28    2.440642    1.407084    1.982613
 29    1.218487    0.706415    1.977456
 30    2.440524    1.407059    1.979097
 31    1.218774    0.706147    1.981616
 32    1.218763    0.706472    1.975667
 33    1.218881    0.706396    1.980487
 34    2.440326    1.406804    1.980241
 35    2.440697    1.406938    1.977788
 36    1.218509    0.706275    1.978579
 37    1.218697    0.706358    1.976640
 38    0.001252    1.406715    1.979160
 39    3.657800    0.706472    1.980058
 40    1.218605    0.706300    1.977567
 41    2.440432    1.406798    1.976411
 42    1.218719    0.706472    1.978171
 43    2.440587    1.407116    1.978722
 44    2.440256    1.406874    1.977252
 45    1.218609    0.706370    1.978172
 46    2.440524    1.406715    1.977881
 47    1.218807    0.706116    1.977505
 48    2.440664    1.407059    1.977973
 49    1.218664    0.706287    1.978164
```

B.3. Reference data of the buckling section

```
wall distance=       2.90000000
rho=       0.10000000
minimal free energy =       0.00106735
name: 2D centered rectangular, a=14.66333 b=2.82196
number density:     0.100000
area density:     0.048333
 number of layers:            6
lattice vectors:
a:     7.466201    0.000000
b:     0.533300    2.771109
inter-layer vectors
  1    2.666501    0.923703    0.000000
  2    2.666501    0.923703    0.000000
  3    5.866301    0.307901    2.900000
  4    2.666501    0.923703    0.000000
  5    2.666501    0.923703    0.000000
-----------------------------------------------
wall distance=       3.00000000
rho=       0.10000000
minimal free energy =       0.00135821
name: 2D centered rectangular, a=14.31698 b=2.79389
number density:     0.100000
area density:     0.050000
 number of layers:            6
lattice vectors:
a:     7.293519    0.000000
b:     0.535119    2.742161
inter-layer vectors
  1    5.182396    1.835268    0.000000
  2    5.237527    1.824509    0.420255
  3    4.175815    0.608404    2.159490
  4    5.237527    1.824510    0.420255
  5    5.182396    1.835268    0.000000
-----------------------------------------------
wall distance=       3.10000000
rho=       0.10000000
minimal free energy =       0.00163349
name: 2D centered rectangular, a=13.93860 b=2.77716
number density:     0.100000
area density:     0.051667
 number of layers:            6
lattice vectors:
a:     7.106286    0.000000
b:     0.542660    2.723622
inter-layer vectors
  1    2.633151    0.891237    0.000000
  2    2.507617    0.916249    0.645797
  3    3.571276    2.120195    1.808406
  4    2.507617    0.916249    0.645797
  5    3.175811    3.614859    0.000000
-----------------------------------------------
wall distance=       3.20000000
rho=       0.10000000
minimal free energy =       0.00189158
name: 2D centered rectangular, a=13.53980 b=2.76961
number density:     0.100000
area density:     0.053333
 number of layers:            6
lattice vectors:
a:     6.910084    0.000000
b:     0.555040    2.713426
inter-layer vectors
  1    4.837833    1.837366    0.000000
  2    5.047108    1.794559    0.833898
  3    3.973114    0.600767    1.532204
  4    5.047108    1.794559    0.833898
  5    4.837833    1.837366    0.000000
-----------------------------------------------
wall distance=       3.25000000
rho=       0.10000000
minimal free energy =       0.00200919
name: 2D centered rectangular, a=13.33305 b=2.76929
number density:     0.100000
area density:     0.054167
 number of layers:            6
lattice vectors:
a:     6.808801    0.000000
b:     0.563166    2.711423
inter-layer vectors
  1    4.744252    1.843006    0.000000
  2    5.001419    1.789592    0.920982
  3    3.917104    0.600609    1.408036
  4    5.001419    1.789592    0.920982
  5    4.744252    1.843006    0.000000
-----------------------------------------------
wall distance=       3.27000000
rho=       0.10000000
minimal free energy =       0.00205349
name: 2D centered rectangular, a=13.24922 b=2.76977
number density:     0.100000
area density:     0.054500
 number of layers:            6
lattice vectors:
a:     6.767817    0.000000
b:     0.566771    2.711158
inter-layer vectors
  1    2.628586    0.865312    0.000000
  2    2.351043    0.923333    0.954812
  3    3.440736    2.110352    1.360377
  4    2.351043    0.923333    0.954812
  5    2.628586    0.865312    0.000000
-----------------------------------------------
wall distance=       3.30000000
rho=       0.10000000
minimal free energy =       0.00209171
name: 2D square, a=3.01511
number density:     0.100000
area density:     0.110000
 number of layers:            3
lattice vectors:
a:     3.015113    0.000000
b:     0.000000    3.015113
inter-layer vectors
  1    1.507557    1.507557    1.650000
  2    1.507557    1.507557    1.650000
```

Bibliography

[1] J. Kepler, *Strena, Seu, de Nive Sexangula* (G. Tampach, Frankfurt, 1611).

[2] N. Steno, *De solido intra solidum naturaliter contento dissertationis prodromus* (Typographia sub signa Stellae, Florence, 1669).

[3] A. Bravais, J. l'Ecole polytechnique **19**, 1 (1850).

[4] W. Bragg, Proceedings of the Cambridge Philosophical Society **17**, 43 (1913).

[5] W. Bragg, Nature **91**, 557 (1913).

[6] S.A. Safran and N.A. Clark, *Physics of Complex and Supermolecular Fluids* (Wiley Interscience, New York, 1987).

[7] R.B. Hunter, *Foundations of Colloid Science* (Clarendon Press, Oxford, 1986).

[8] W.B. Russel, D.A. Saville, and W.R. Schowalter, *Colloidal Dispersions* (Cambridge University Press, Cambridge, 1989).

[9] C.N. Likos, Phys. Rep. **348**, 267 (2001).

[10] P.J. Flory and W.R. Krigbaum, J. Chem. Phys. **18**, 1086 (1950).

[11] C.N. Likos, N. Hoffmann, H. Löwen, and A.A. Louis, J. Phys.: Condens. Matter **14**, 7681 (2002).

[12] J.G. Kirkwood, J. Chem. Phys. **18**, 380 (1950).

[13] W.W. Wood, J. Chem. Phys. **20**, 1334 (1952).

[14] A. Bonissent, P. Pieranski, and P. Pieranski, Philos. Mag. A **50**, 57 (1984).

[15] K.W. Wojciechowski, Phys. Rev. A **122**, 377 (1987).

[16] D. Oxtoby, in *Les Houches, Session LI, Liquids, Freezing and Glass Transition*, edited by J.-P. Hansen, D. Levesque, and J. Zinn-Justin (North-Holland, Amsterdam, 1991).

[17] Y. Singh, Phys. Rep. **207**, 351 (1991).

[18] A.D.J. Haymet, in *Fundamentals of Inhomogeneous Liquids*, edited by D. Henderson (Marcel-Dekker, New York, 1992).

[19] H. Löwen, Phys. Rep. **237**, 249 (1994).

[20] M. Schmidt, J. Phys.: Condens. Matter **15**, 101 (2003).

[21] M. Garey and D. Johnson, *Computers and Intractability: A Guide to the Theory of NP-Completeness* (Freeman, New York, 1979).

[22] D. Gottwald, Ph.D. thesis, TU Vienna, 2005.

[23] D. Gottwald, C.N. Likos, G. Kahl, and H. Löwen, Phys. Rev. Lett. **92**, 068301 (2004).

[24] M. Watzlawek, C. Likos, and H. Löwen, Phys. Rev. Lett. **82**, 5289 (1999).

[25] G. Pauschenwein and G. Kahl, Soft Matter, D01:10.1039/bb06147e, 2008.

[26] V. Balagurusamy, G. Ungar, V. Percec, and G. Johansson, J. Am. Chem. Soc. **119**, 1539 (1997).

[27] G. McConnell and A. Gast, Macromolecules **30**, 435 (1997).

[28] B. Pansu, P. Pieranski, and P. Pieranski, J. Phys. (Paris) **45**, 331 (1984).

[29] S. Neser, C. Bechinger, P. Leiderer, and T. Palberg, Phys. Rev. Lett. **79**, 2348 (1997).

[30] B. Krüger, L. Schärfer, and A. Baumgärtner, J. Physique **50**, 3191 (1989).

[31] F. Stillinger, J. Chem. Phys. **65**, 3968 (1976).

[32] F. Stillinger, Phys. Rev. B **20**, 299 (1979).

[33] F. Stillinger and D. K. Stillinger, Physica A **244**, 358 (1997).

[34] A. Lang, C.N. Likos, M. Watzlawek, and H. Löwen, J. Phys.: Condens. Matter **12**, 5087 (2000).

[35] C. Darwin, *The Origin of Species by Means of Natural Selection* (John Murray, Albemarle Street, London, 1859).

[36] J.H. Holland, *Adaption in Natural and Artificial Systems* (The University of Michigan Press, Ann Arbor, 1975).

[37] D.E. Goldberg, *Genetic Algorithms in Search, Optimization and Machine Learning* (Addison-Wesley, MA, 1989).

[38] Z. Michalewicz, *Genetic Algorithms + Data Structures = Evolution Programs* (Springer, New York, 1992).

[39] C. To and J. Vohradsky, BMC Genomics **8**, 49 (2007).

[40] E. Cantu-Paz, *Efficient and Accurate Parallel Genetic Algorithms (Vol 1)* (Springer, New York, 2000).

[41] W. Stemmer, Nature **370**, 389 (1994).

[42] A. Assioen, Science **282**, 919 (1998).

[43] D.H. Deaven and K.M. Ho, Phys. Rev. Lett. **75**, 288 (1995).

[44] I. Rechenberg, *Evolutionsstrategie* (Friedrich Frommann Verlag, Stuttgart, 1973).

[45] I. Rechenberg, Evolutionsstrategie '92, 1992, unveröffentlichtes Manuskript.

[46] J.P. Hansen and I.R. McDonald, *Theory of Simple Liquids*, 2nd ed. (Academic Press, London, 1986).

[47] D. Chandler, *Introduction to Modern Statistical Mechanics* (Oxford University Press, New York, 1987).

[48] G. Pauschenwein, Ph.D. thesis, TU Vienna, 2008.

[49] W. Press, S. Teukolsky, W. Vetterling, and B. Flannery, *Numerical Recipes in C: The Art of Scientific Computing, Second Edition* (Cambridge University Press, New York, 1992).

[50] P. Pieranski, L. Strzelecki, and B. Pansu, Phys. Rev. Lett. **50**, 900 (1983).

Danksagung

Während meines Studiums und im Speziellen während dieser Arbeit wurde ich von einer Anzahl von Menschen immer wieder auf unterschiedlichste Weise unterstützt. Durch sie ist all das erst möglich geworden. Es ist an der Zeit Danke zu sagen:

Besonderer Dank gilt meinem Betreuer Gerhard Kahl, für seine Unterstützung, Freundlichkeit und im Besonderen für dessen Ermutigungen, welche meine Selbstzweifel immer wieder zu zerstreuen vermochten.

Für wertvolles Feedback und Ratschläge möchte ich Jean-Jacques Weis aus Paris sowie Christos Likos aus Düsseldorf danken.

Meinen Kollegen Julia Fornleitner, Bianca Mladek, Maria-José Fernaud sowie Gernot Pauschenwein, Dieter Schwanzer, Daniele Coslovich, Jan Kurzidim und Georg Falkinger danke ich für die herzliche Aufnahme in die Arbeitsgruppe und für die geduldige Beantwortung all meiner Fragen.

Großer Dank gilt meinen Studienkollegen Manfred Schuster, Stefan Nagele, Martin Willitsch, Reinhard Wehr, Roman Kogler sowie Cosima Koch und Veronika Schweigel für die freundschaftliche Begleitung einer intensiven Zeit, die wertvollen Diskussionen über Gott und die Welt und auch für die nicht missen wollenden unzähligen tollen Parties.

Ich danke Andre Guggenberger für die langjährige Freundschaft, die kritischen Diskussionen und fr die vielen gemeinsam erlebten Abenteuern.

Meinen Eltern Doris und Hermann Kahn möchte ich ganz besonders danken, für die seelische Unterstützung, den finanziellen Rückhalt, das moralische Rüstzeug und für ihr immerwährendes Vertrauen in meine Fähigkeiten.

Größtmöglicher Dank gilt Yvonne für ihre Liebe und Geduld sowie für den nicht endenwollenden Glauben an mich.

Man darf schweigen.
Die guten Dinge sind getan, offenbar.
Alexander Widner
Tag und Nacht und Tag